BASICS OF IN VIVO X-NUCLEAR MRS

Lijing Xin

CIBM EPFL MRI

10.04.2025

Lijing.xin@epfl.ch

PROPERTIES OF OTHER NUCLEI BEYOND ^{1}H

CIBM Center for Biomedical Imaging

- Metabolite levels
- Physiological parameters
- Kinetics in metabolic pathways
- Endogenous tracer (^{31}P MRS)
- Exogenous tracers (nuclei with low natural abundance)

Isotope	Spin I^a	Natural abundance	γ $(10^6 rad \cdot s^-1T^{-1})$
^{1}H	1/2	0.99985	267.522
^{2}H	1	0.00015	41.066
^{12}C	0	0.989	–
^{13}C	1/2	0.01108	67.283
^{14}N	1	0.9963	19.338
^{15}N	1/2	0.0037	-27.126
^{16}O	0	0.99963	–
^{17}O	5/2	0.00037	-36.279
^{23}Na	3/2	1	70.801
^{31}P	1/2	1	108.394

Low natural abundance

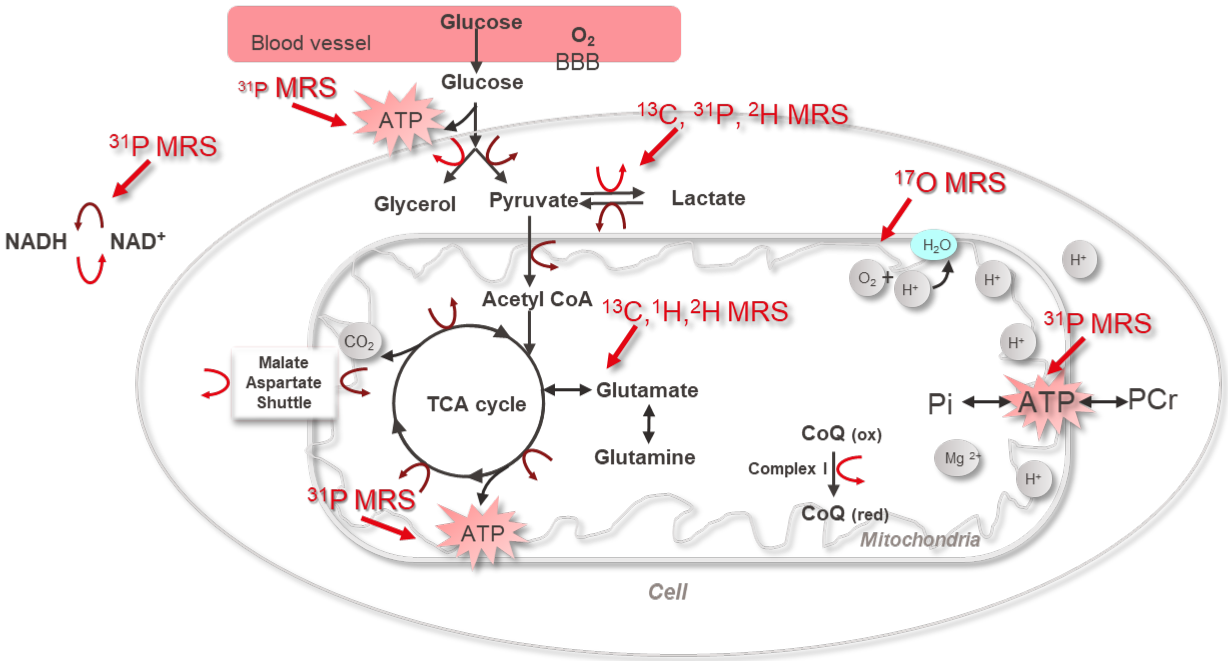

© CIBM | Center for Biomedical Imaging

^{31}P MRS

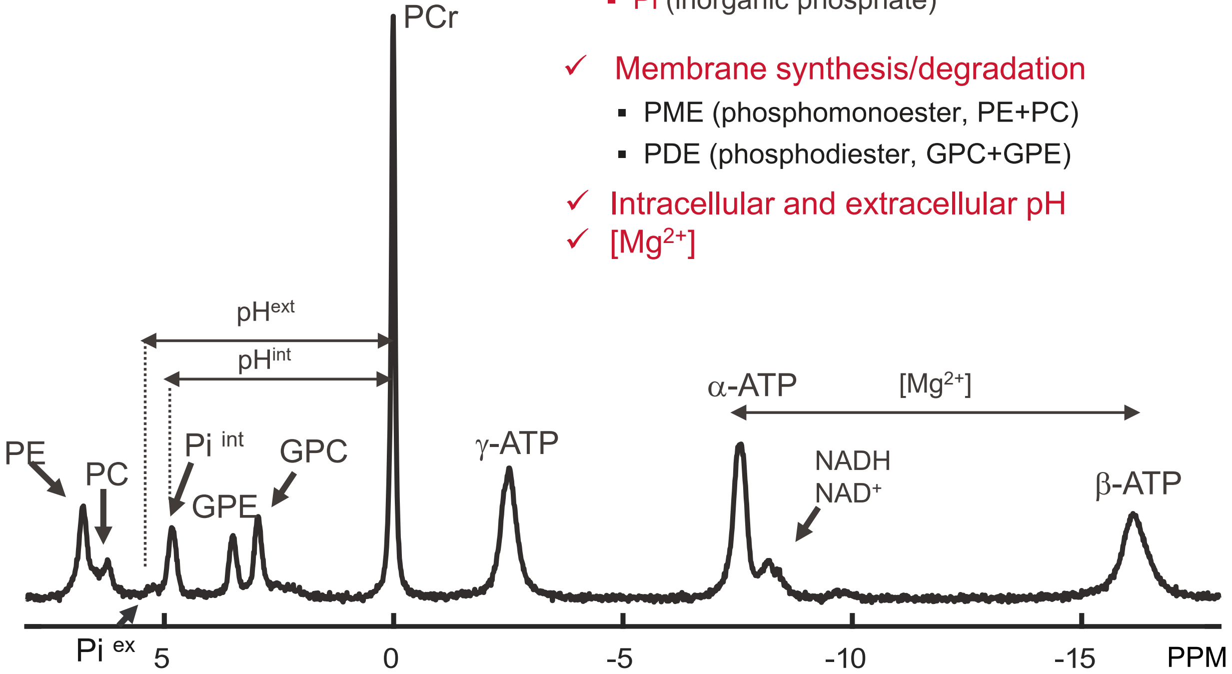

- ✓ Energy metabolites
  - ATP (adenosine triphosphate)
  - PCr (phosphocreatine)
  - Pi (inorganic phosphate)
- ✓ Membrane synthesis/degradation
  - PME (phosphomonoester, PE+PC)
  - PDE (phosphodiester, GPC+GPE)
- ✓ Intracellular and extracellular pH
- ✓ [Mg^{2+}]

- ✓ Nicotinamide adenine dinucleotide (NAD^{+}/NADH)

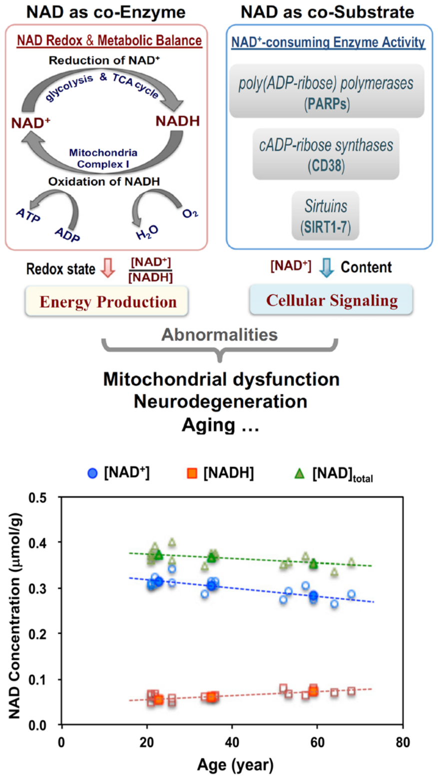

Zhu et al., PNAS, (2015)

© CIBM | Center for Biomedical Imaging

LOCALIZATION FOR ^{31}P MRS

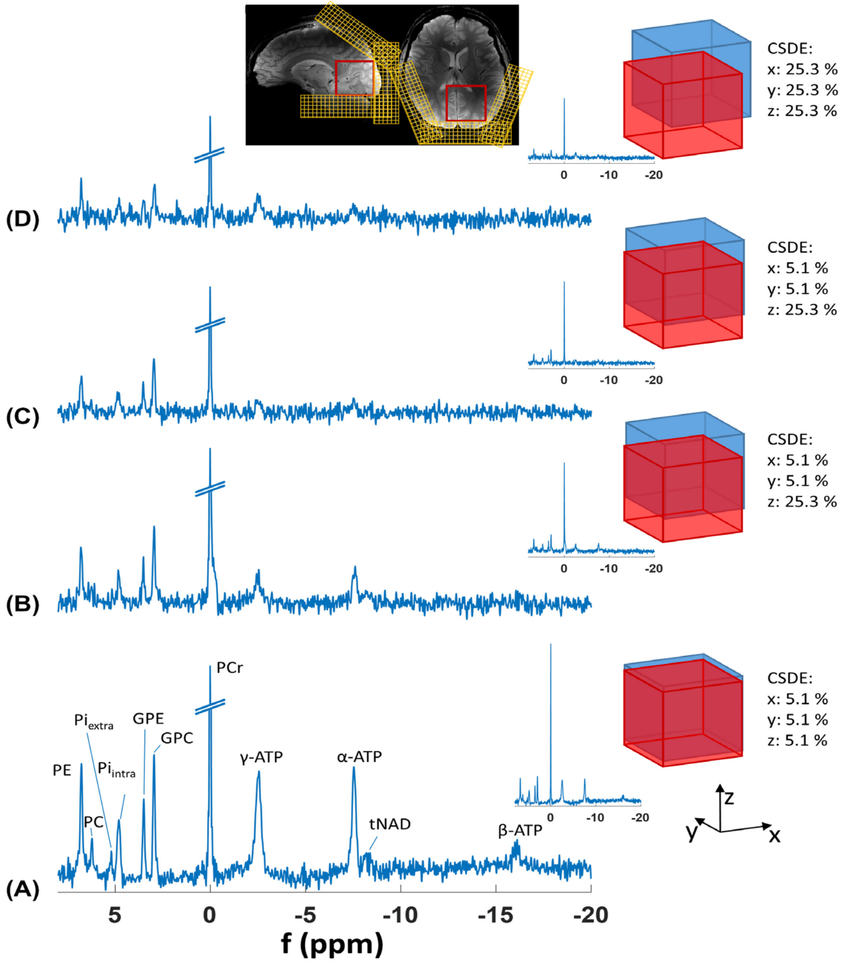

Comparison of four 31P single-voxel MRS sequences in the human brain at 9.4 T

	Meta.	References
T_1 [s]	PCr	3.37-3.39 (6; 7)
	Pi	3.19-3.70 (6; 7)
	γATP	1.27-1.70 (6; 7)
	αATP	1.26-1.35 (6; 7)
	βATP	1.02-1.13 (6; 7)
T_2 [ms]	PCr	132.0 $\pm$ 12.8 (6)
	Pi	86 $\pm$ 2 (8)
	γATP	26.1 $\pm$ 9.6 (6)
	αATP	25.8 $\pm$ 6.6 (6)
	βATP	-

Relaxation times of 31P metabolites at 7T

T2 of ^{1}H metabolites: 60-200ms

CIBM.CH

Dorst et al., MRM, 2021

© CIBM | Center for Biomedical Imaging

^{31}P MRS

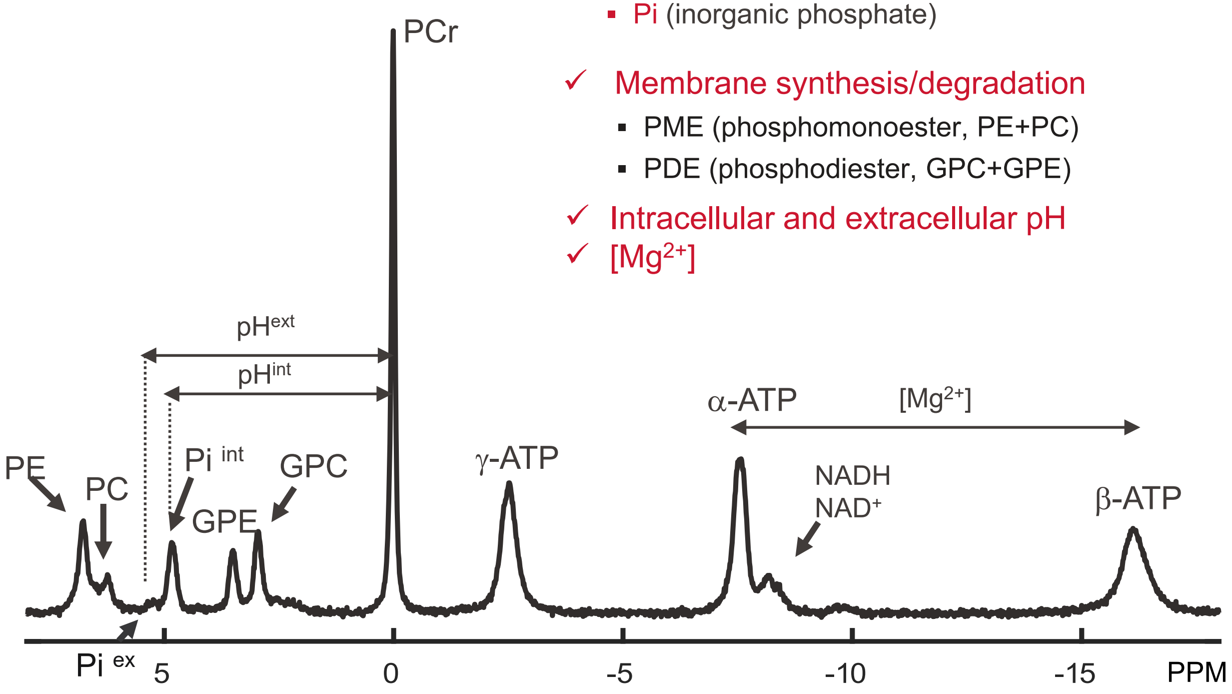

- ✓ Energy metabolites
  - ATP (adenosine triphosphate)
  - PCr (phosphocreatine)
  - Pi (inorganic phosphate)
- ✓ Membrane synthesis/degradation
  - PME (phosphomonoester, PE+PC)
  - PDE (phosphodiester, GPC+GPE)
- ✓ Intracellular and extracellular pH
- ✓ [Mg^{2+}]

- ✓ Nicotinamide adenine dinucleotide (NAD^{+}/NADH)

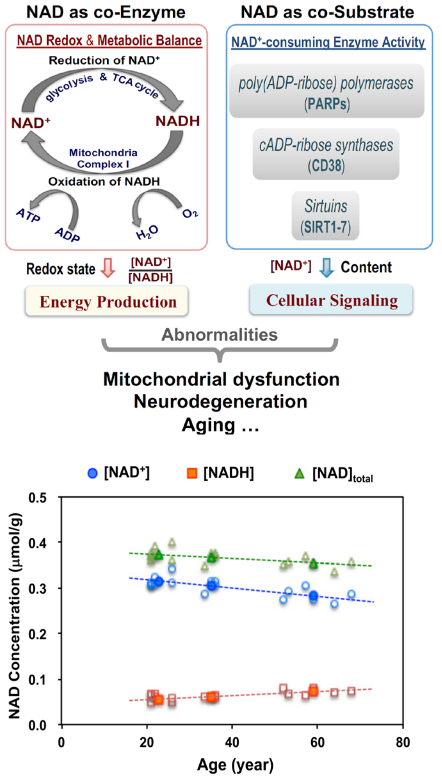

Zhu et al., PNAS, (2015)

- ✓ ATP metabolism

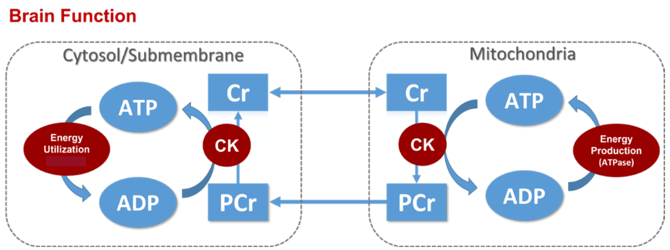

CIBM.CH

WHY MEASURE ATP METABOLISM

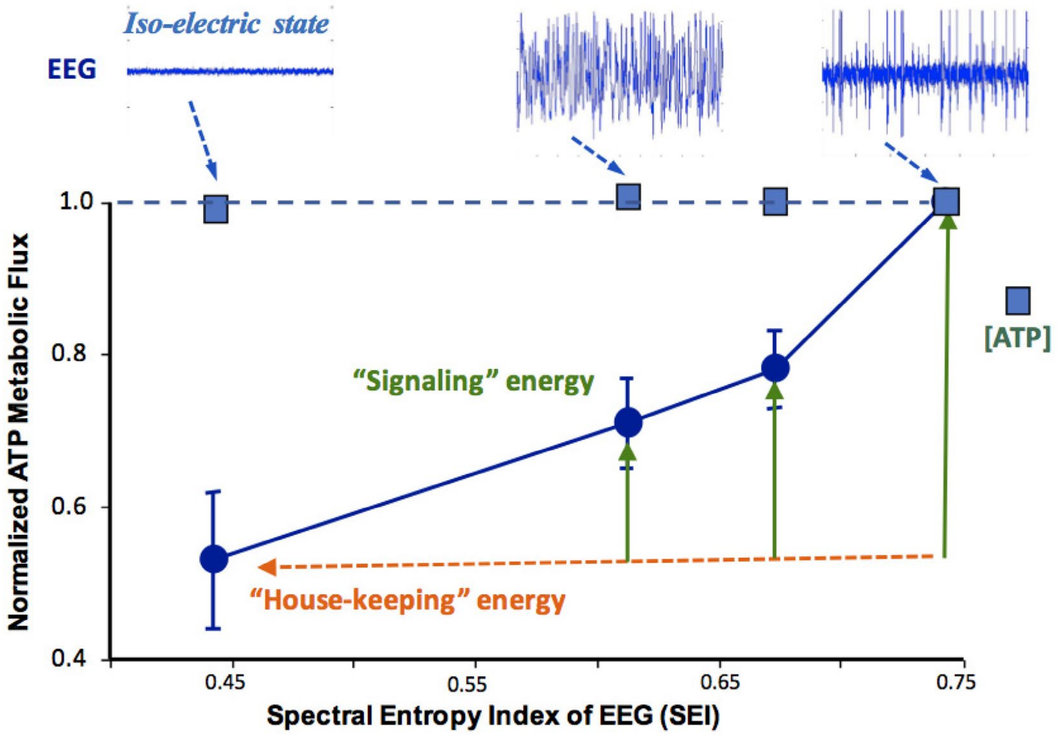

Zhu et al., Frontiers in Aging Neuroscience (2018)

Table 2. Results of [31]P Magnetization Transfer Spectroscopy Measurements in the Human Frontal Lobe of Patients With Schizophrenia (SZ) and Healthy Control (HC) Subjects

Variable	Mean (SD) SZ (n = 26)	Mean (SD) HC (n = 26)	P Value
Magnetization ratio			
Phosphocreatine to β-ATP	1.35 (0.24)	1.36 (0.17)	.71
Inorganic phosphate to β-ATP	0.44 (0.09)	0.42 (0.07)	.47
Phosphodiester to β-ATP	0.91 (0.19)	1.05 (0.19)	.02
Phosphomonoester to β-ATP	1.05 (0.14)	1.09 (0.16)	.54
Intracellular pH	7.00 (0.02)	7.03 (0.01)	.007[a]
M_s:M_0 ratio of phosphocreatine[b]	0.50 (0.12)	0.43 (0.07)	.01
Rate constant k_f of creatine kinase, s^{-1}	0.21 (0.07)	0.27 (0.06)	.003
Intrinsic longitudinal T_1 relaxation time of phosphocreatine, s	5.21 (1.24)	5.03 (1.09)	.67
Chemical exchange flux of creatine kinase, μmol/g/min	49.93 (21.95)	61.43 (16.08)	.03
Magnesium ion concentration, mmol/L	0.149 (0.026)	0.145 (0.027)	.59

Du et al., JAMA Psychiatry (2014)

© CIBM | Center for Biomedical Imaging

ATP metabolism by ^{31}P magnetization transfer

Saturation transfer

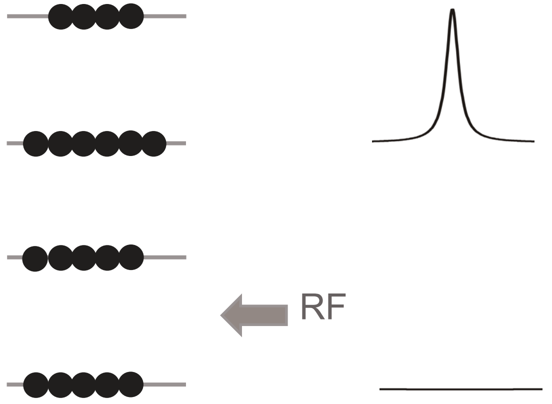

Saturation: equalize the population of energy state

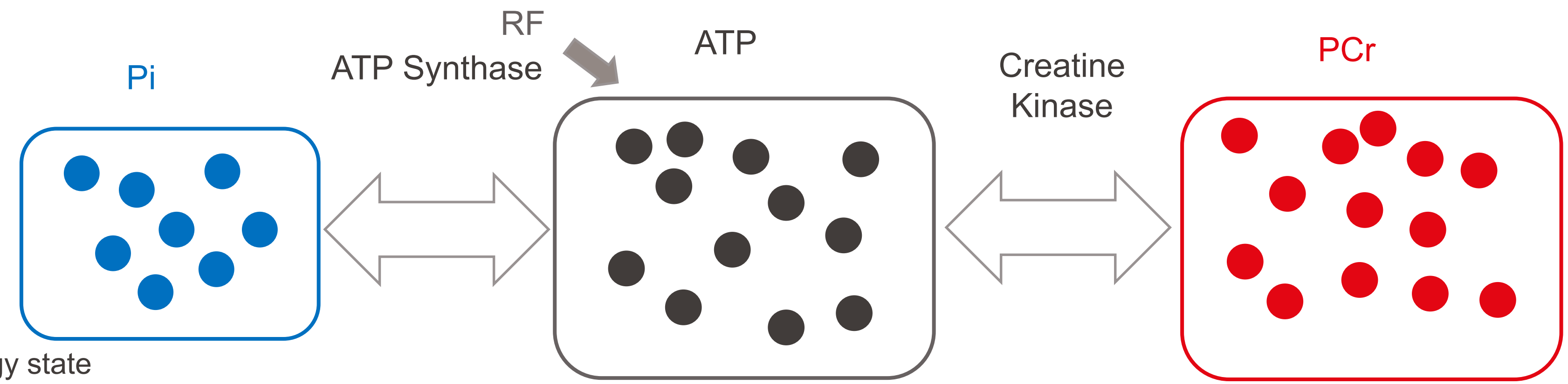

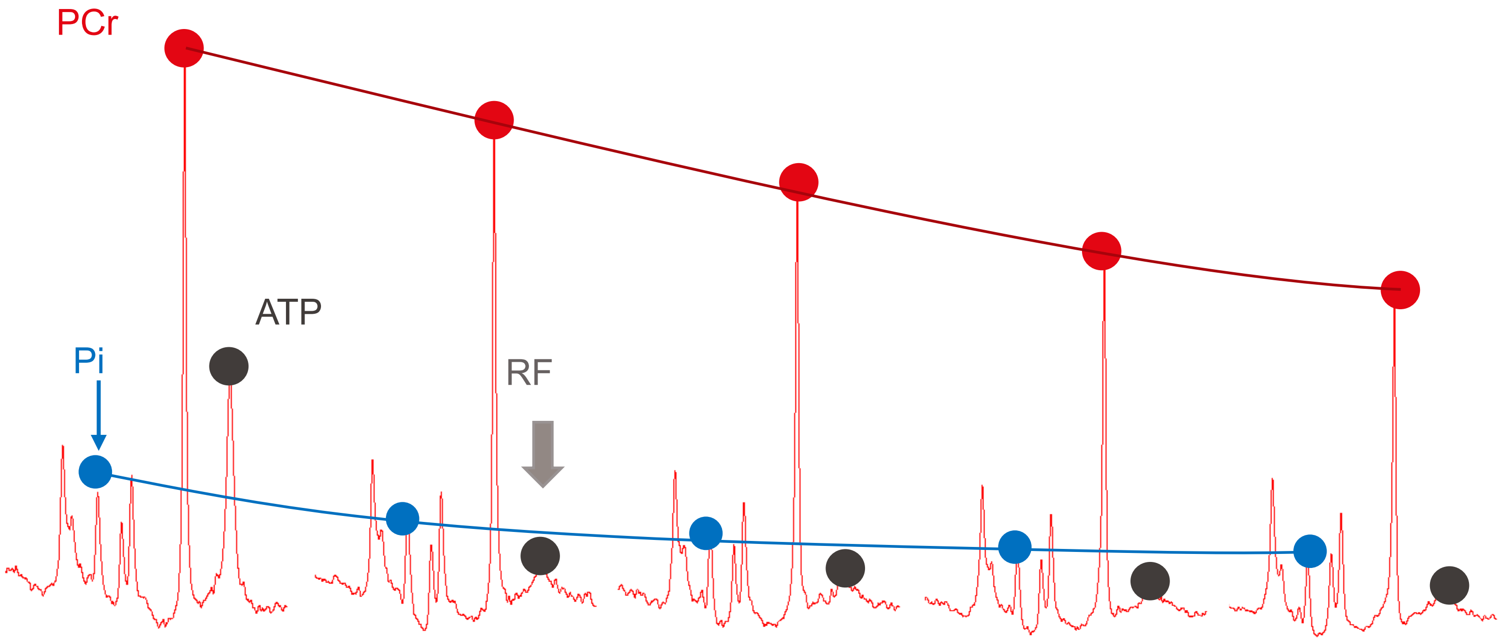

$$\underset{\mathbf{a}}{\text{PCr}} \underset{k_{-1}}{\overset{k_1}{\rightleftarrows}} \underset{\mathbf{b}}{\gamma\text{-ATP}} \underset{k_2}{\overset{k_{-2}}{\leftrightarrows}} \underset{\mathbf{c}}{\text{P}_\text{i}}$$

$$\frac{dM_a}{dt} = -\frac{(M_a - M_a^0)}{T_{1a}} - k_1 M_a + k_{-1} M_b \qquad [1a]$$

$$\frac{dM_b}{dt} = -\frac{(M_b - M_b^0)}{T_{1b}} - k_{-1} M_b - k_2 M_b + k_1 M_a + k_{-2} M_c \qquad [1b]$$

$$\frac{dM_c}{dt} = -\frac{(M_c - M_c^0)}{T_{1c}} - k_{-2} M_c + k_2 M_b \qquad [1c]$$

Du et al., MRM, (2007).

DYNAMIC X-NUCLEI MRS: METABOLIC FLUX

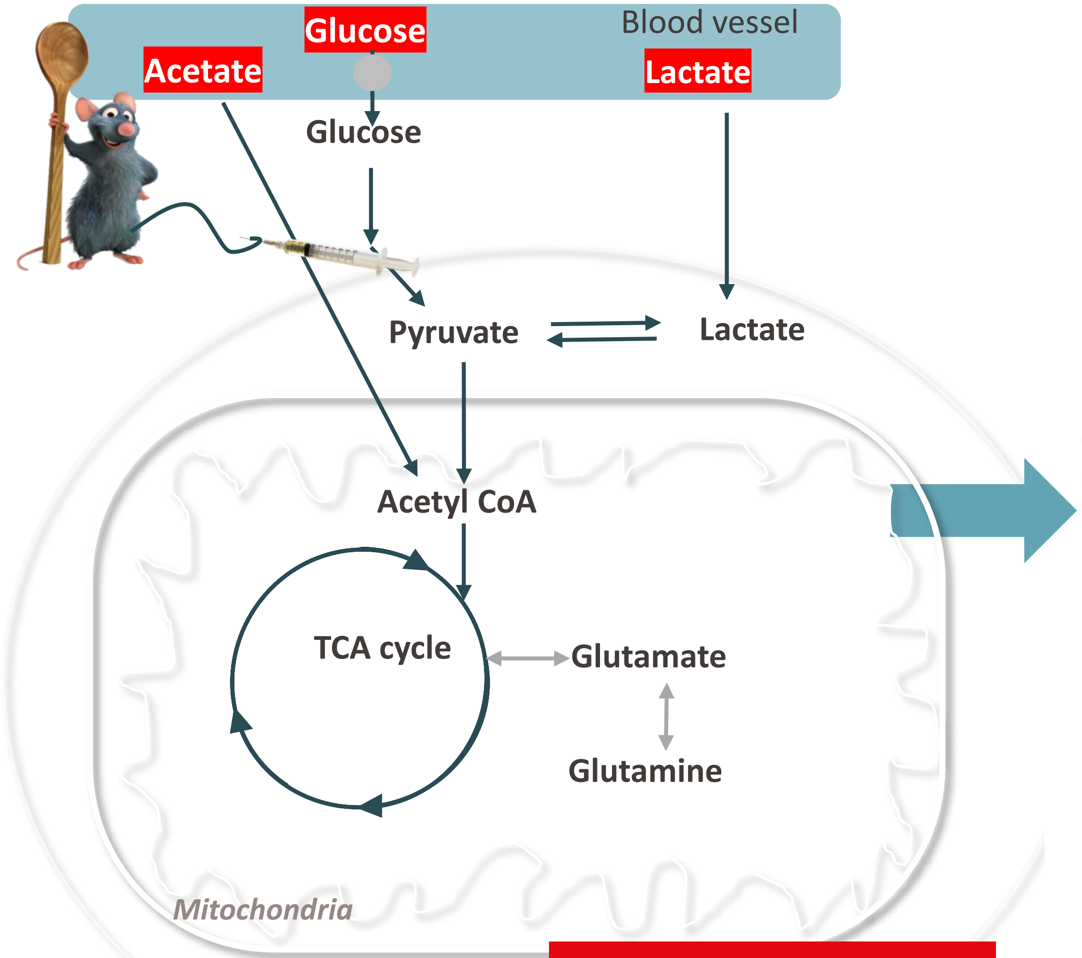

infusion labeled substrate (e.g.^{13}C , ^{2}H)

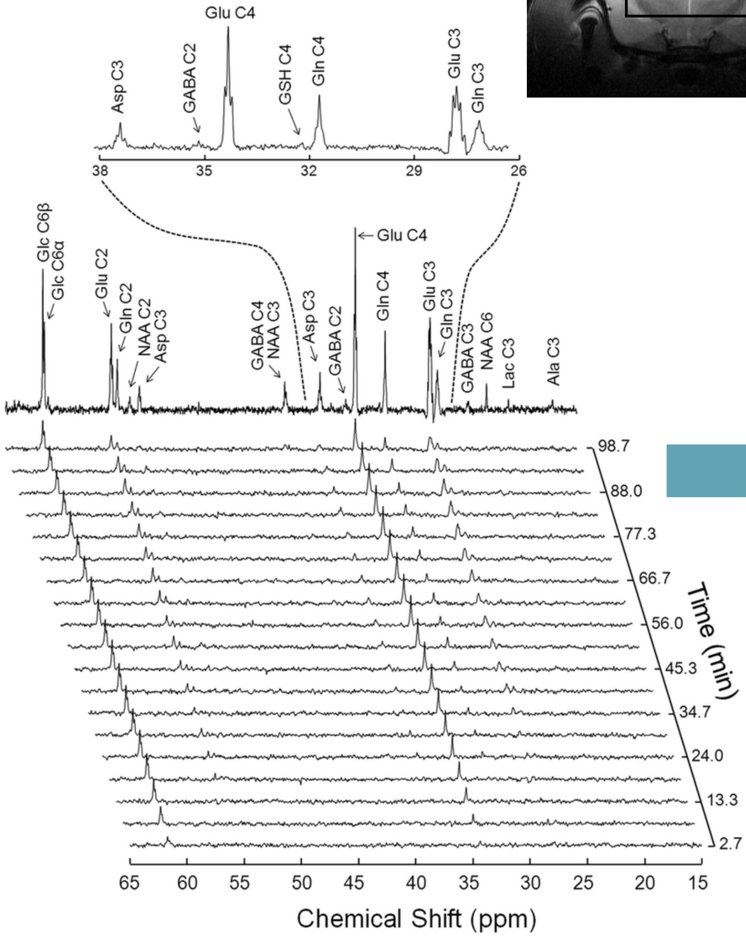

probe labeling time course

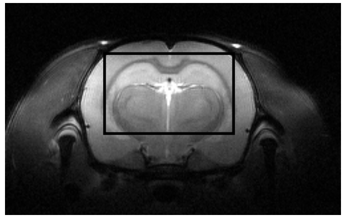

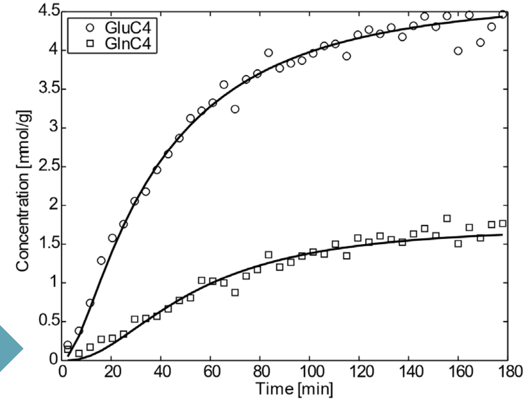

$$\frac{d[P^*]}{dt} = \frac{[S^*]}{[S]} V_1 - \frac{[P^*]}{[P]} V_2$$

neuron TCA flux (V_{TCAn})
glial TCA flux (V_{TCAg})
Glu-Gln cycling flux (V_{NT})

mathematic modelling (metabolic fluxes)

© CIBM | Center for Biomedical Imaging

^{2}H MRS – DYNAMIC METABOLIC STUDY

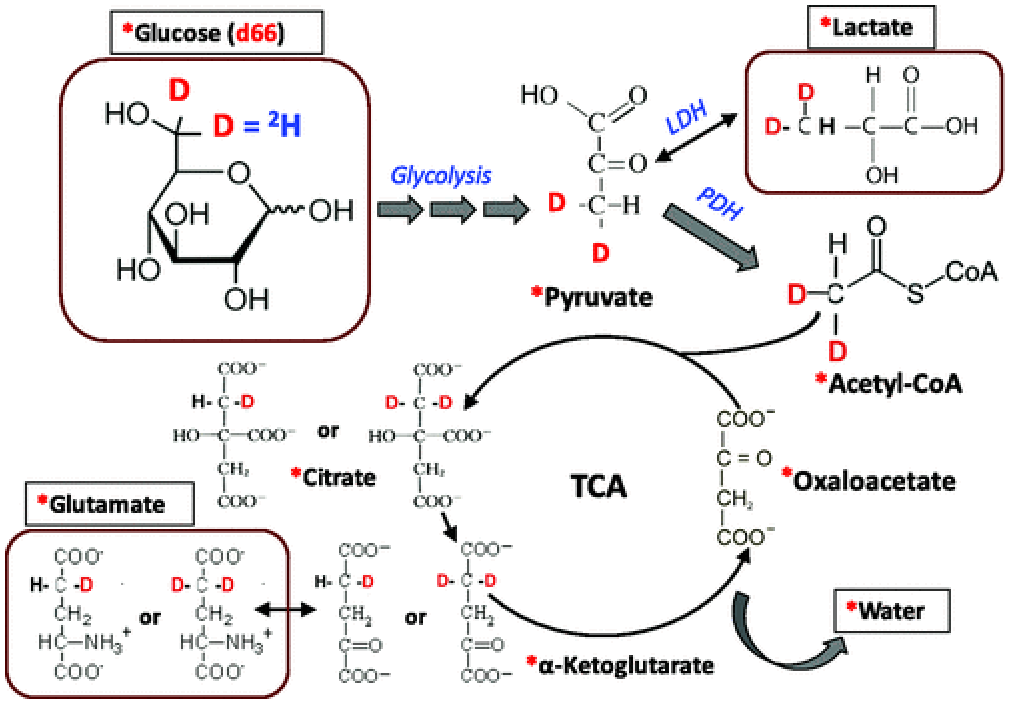

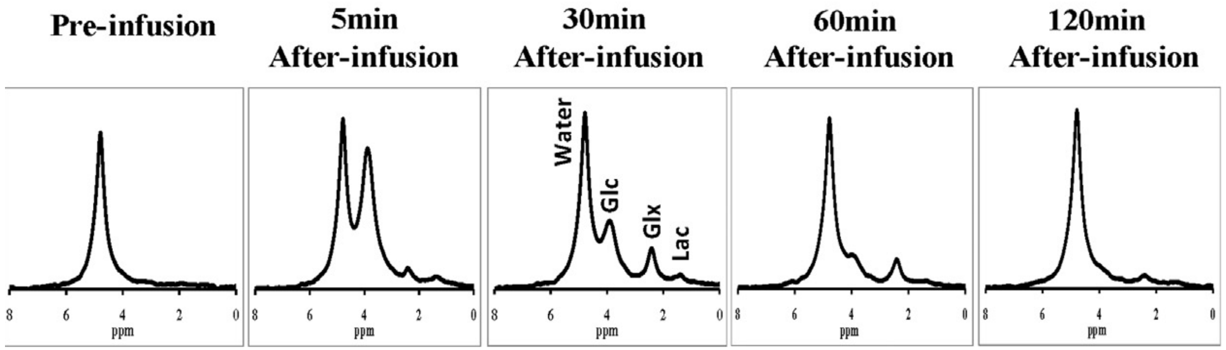

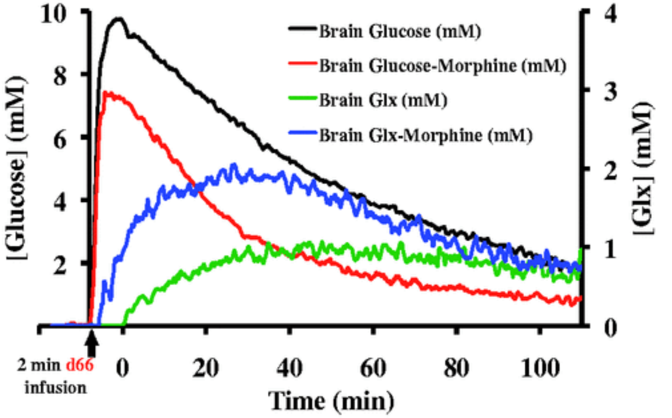

CMR_{glc}

V_{TCA}

Lu et al., JCBFM (2017)

© CIBM | Center for Biomedical Imaging

^{2}H MRS – SIMPLE AND ROBUST

- Short T_1 (100-400ms): fast averaging, sensitivity gain
- Short T_2 (30-60ms): broad resonances
  - Gln+Glu, problem for Glu-Gln cycling flux
  - Insensitive to B_0 inhomogeneity
- Low natural abundance: no water and fat suppression required

Isotope	Spin I^a	Natural abundance
^{1}H	1/2	0.99985
^{2}H	1	0.00015
^{12}C	0	0.989
^{13}C	1/2	0.01108
^{14}N	1	0.9963
^{15}N	1/2	0.0037
^{16}O	0	0.99963
^{17}O	5/2	0.00037
^{23}Na	3/2	1
^{31}P	1/2	1

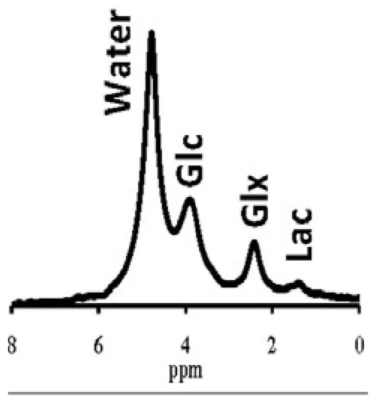

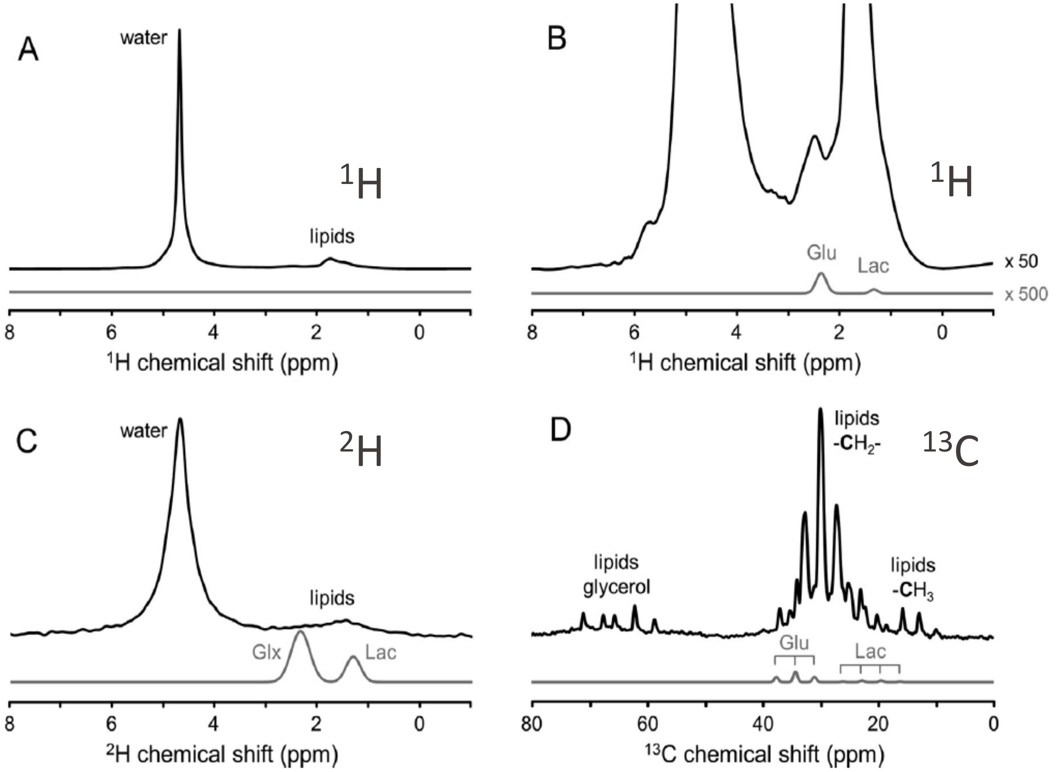

De Feyter et al., JMR (2021)

3D 2H MRSI

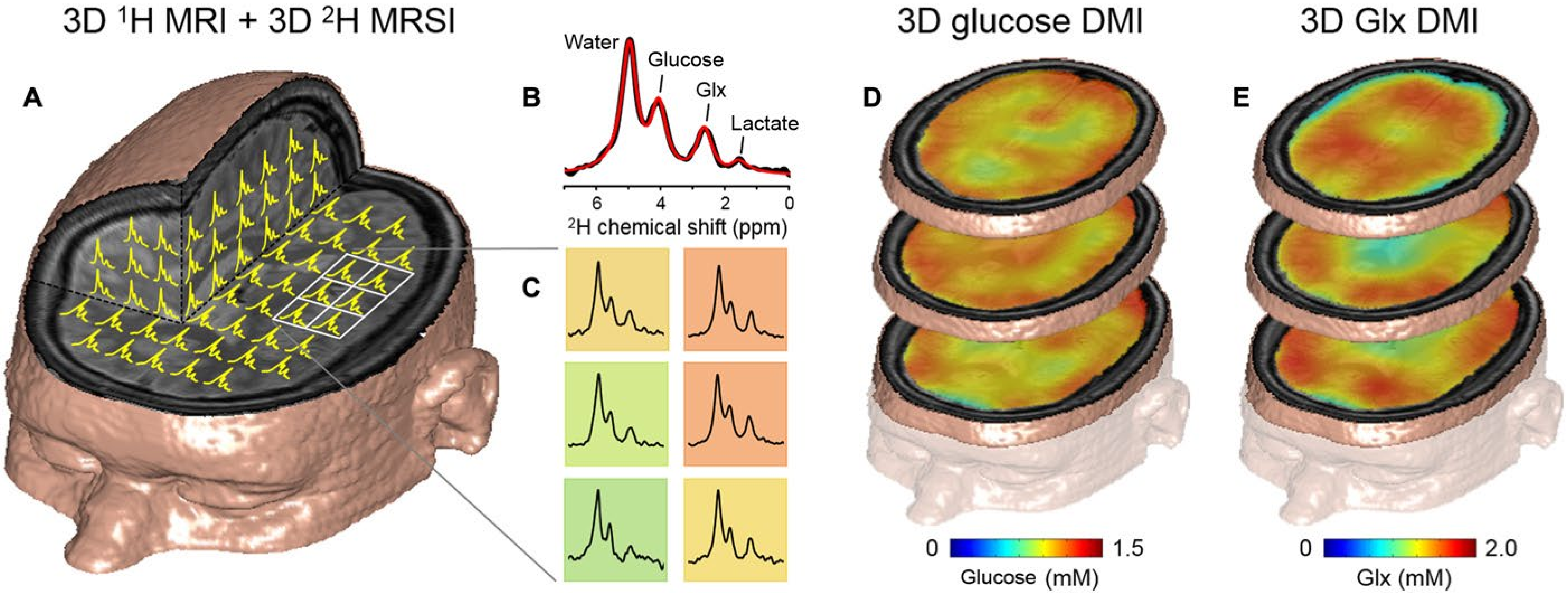

3D FID-MRSI data set: 20 × 20 × 20 mm^3 nominal spatial resolution, TR = 333ms, 29min, acquired between 65 and 90 min after oral [6,6′-$^2H_2$]glucose administration.

De Feyter et al, Sci. Adv. (2018).

© CIBM | Center for Biomedical Imaging

2H MRS APPLICATION IN BRAIN TUMOR

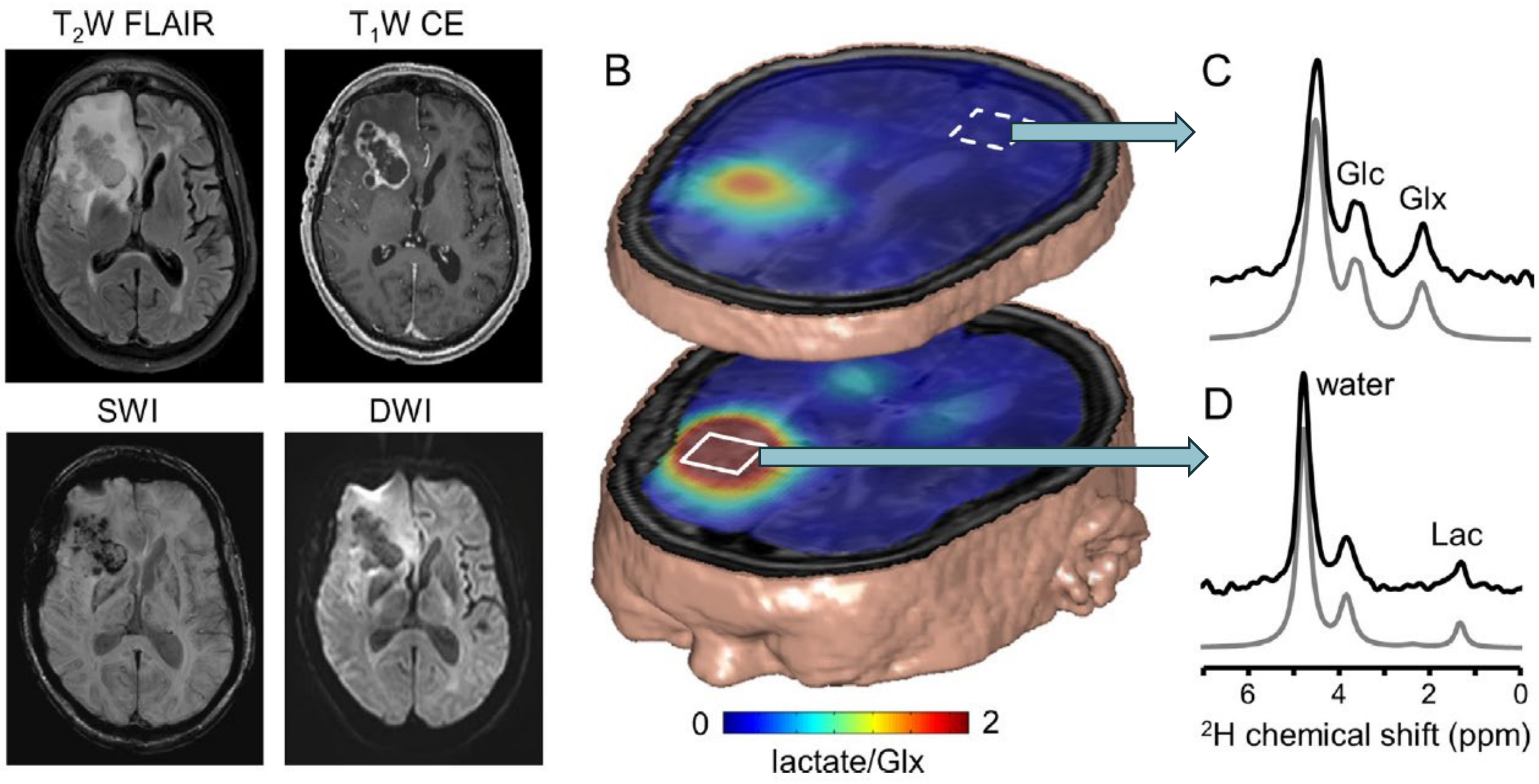

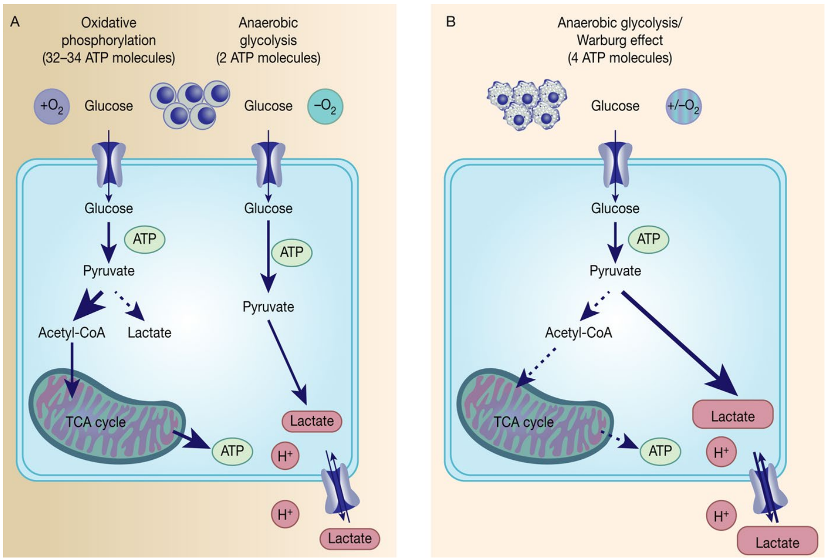

De Feyter et al, Sci. Adv. (2018).
Unterlass JE, Curtin NJ.(2019)

^{13}C MRS – DYNAMIC METABOLIC STUDY

^{2}H MRS

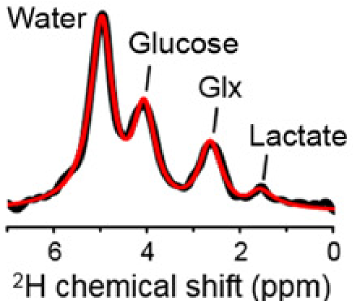

CMR_{Glc}
V_{TCA}
CMR_{LAC}

^{13}C MRS

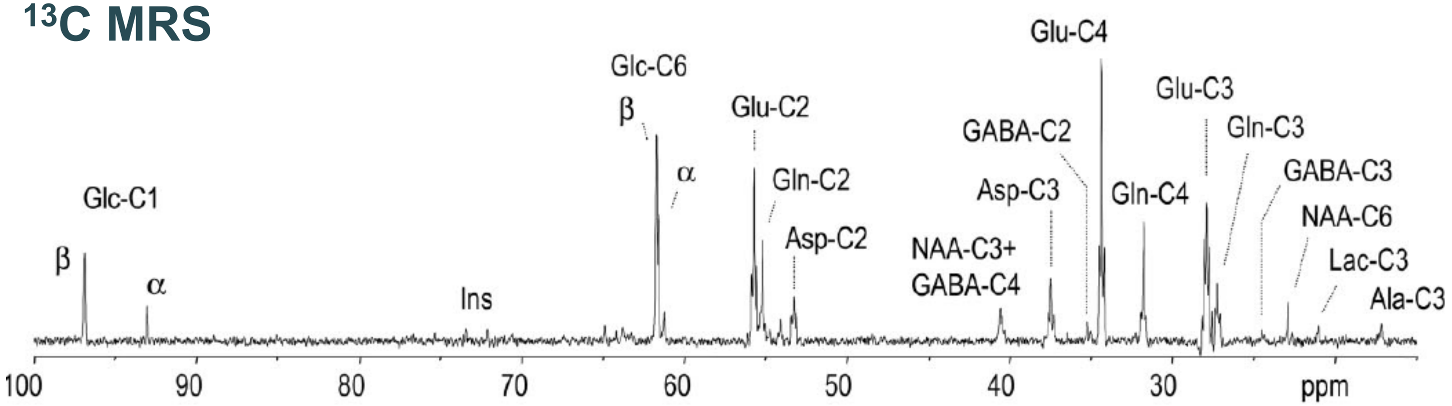

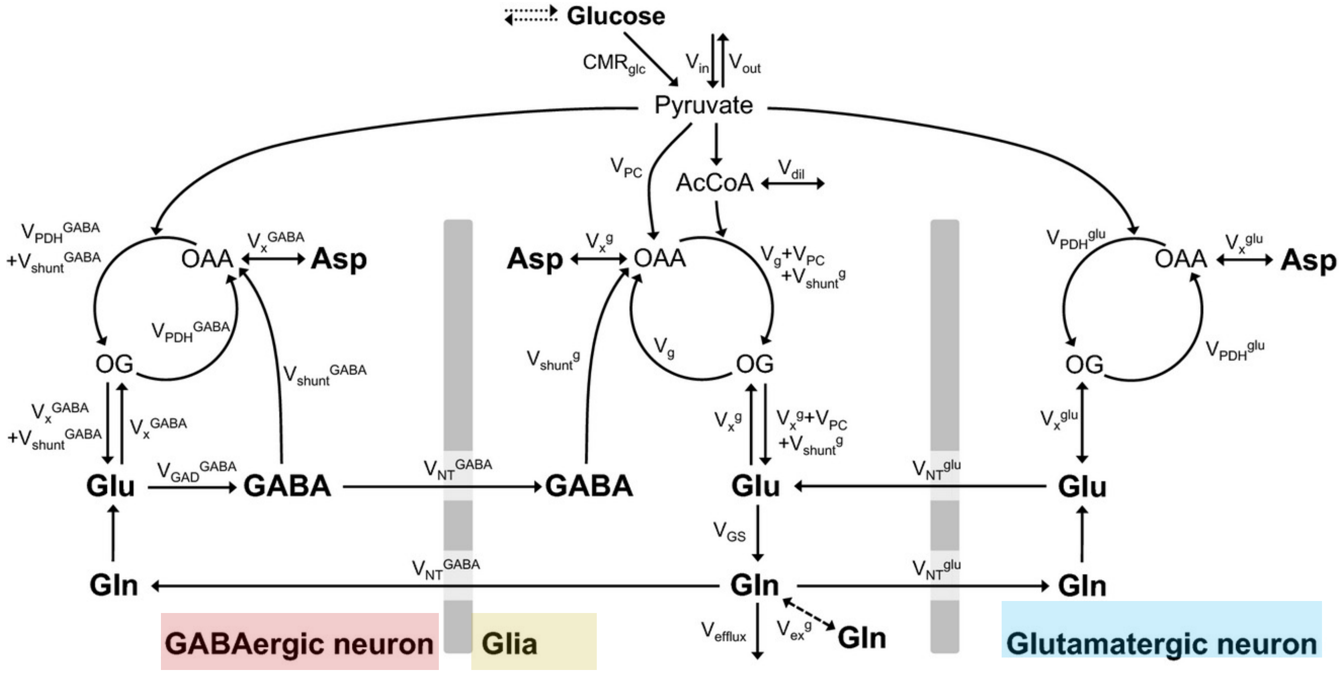

- **Abundant metabolic information**
- **Complexity in acquisition**

Duarte & Gruetter J Neurochem (2013).

© CIBM | Center for Biomedical Imaging

^{13}C MRS – DIFFERENT SUBTRATES

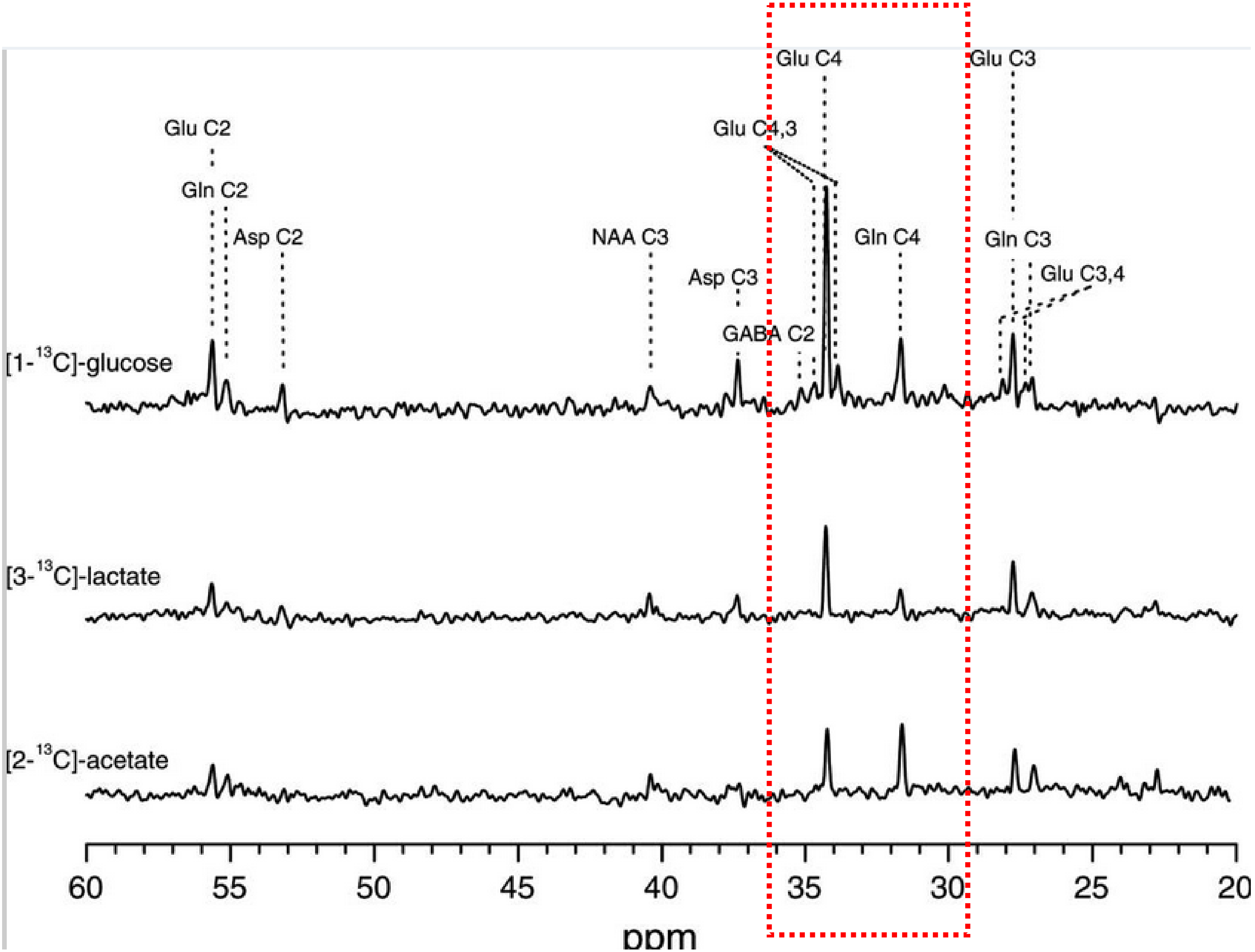

last 18 min of a 2-hour [1-^{13}C] glucose, [3-^{13}C] lactate or [2-^{13}C] acetate infusion

© CIBM | Center for Biomedical Imaging

SENSITIVITY ENHANCEMENT

$\gamma\,(^1H) \sim 4\,\gamma\,(^{13}C)$

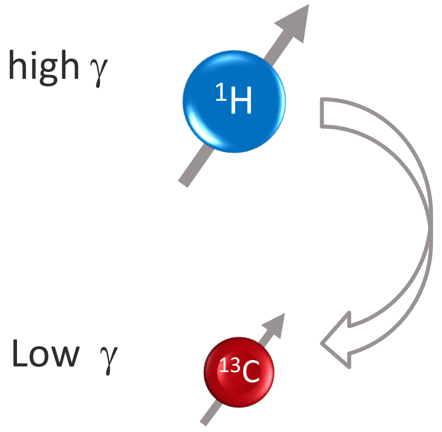

- Decoupling
- NOE: Nuclear Overhauser Enhancement
- Polarization transfer (x 4)
- Heteronuclear editing (Indirect detection ^1H-[^{13}C], x 16)

$$\mathbf{M}_0 = N_s \frac{\gamma^2 \hbar^2 B_0}{4kT}\mathbf{k}$$

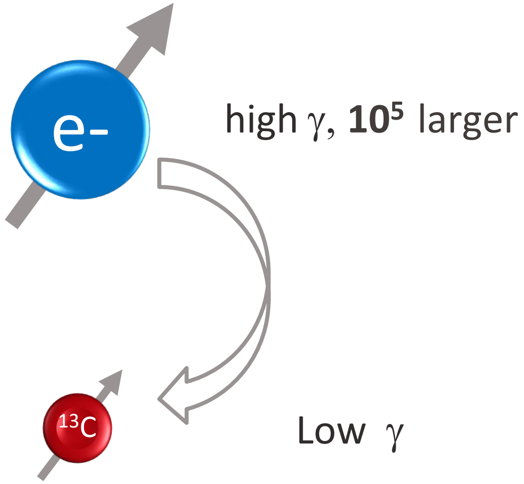

- Hyperpolarization (DNP, x 10000)

DECOUPLING

- Why decoupling?   simplify spectra and enhance SNR

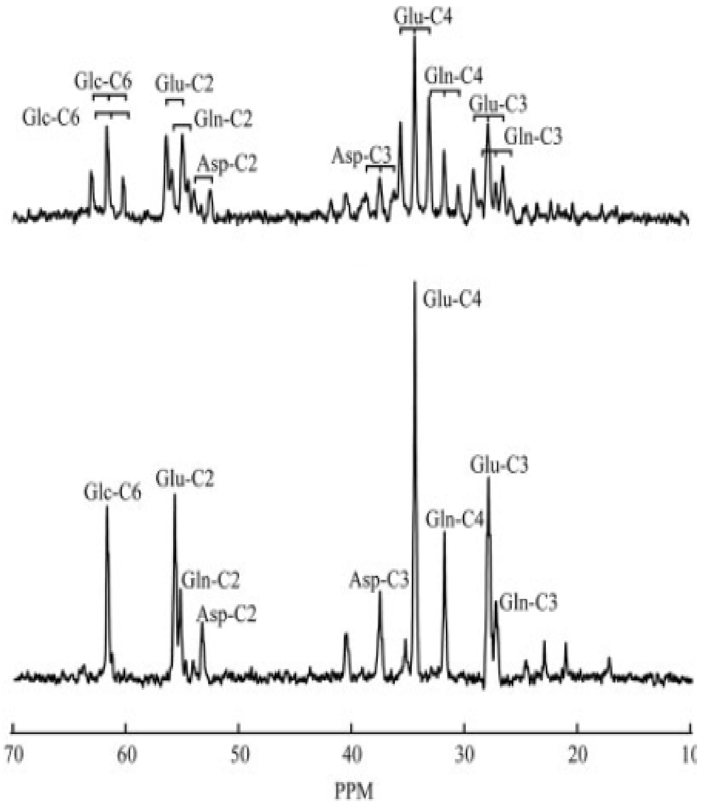

undecoupled

decoupled

Deelchand, et al , Magn Reson Med, 55,2006

HOW TO DO DECOUPLING?

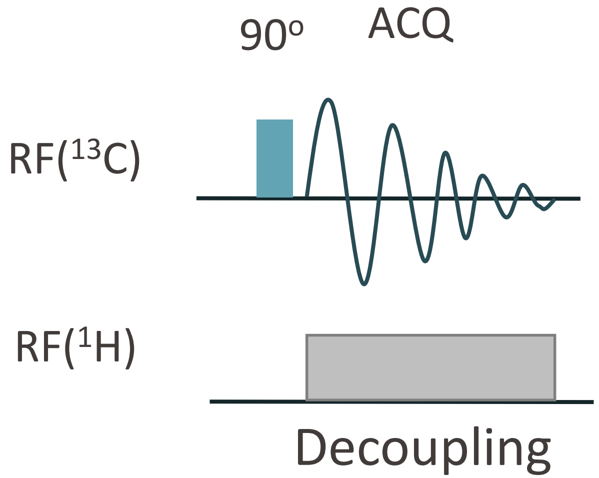

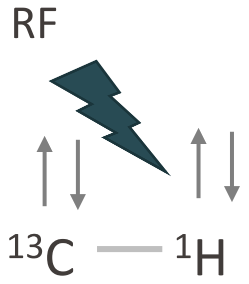

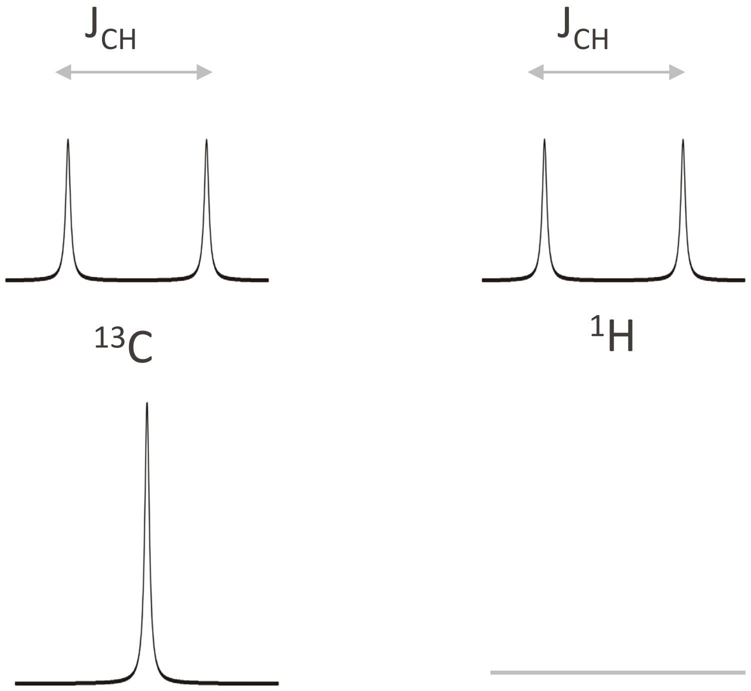

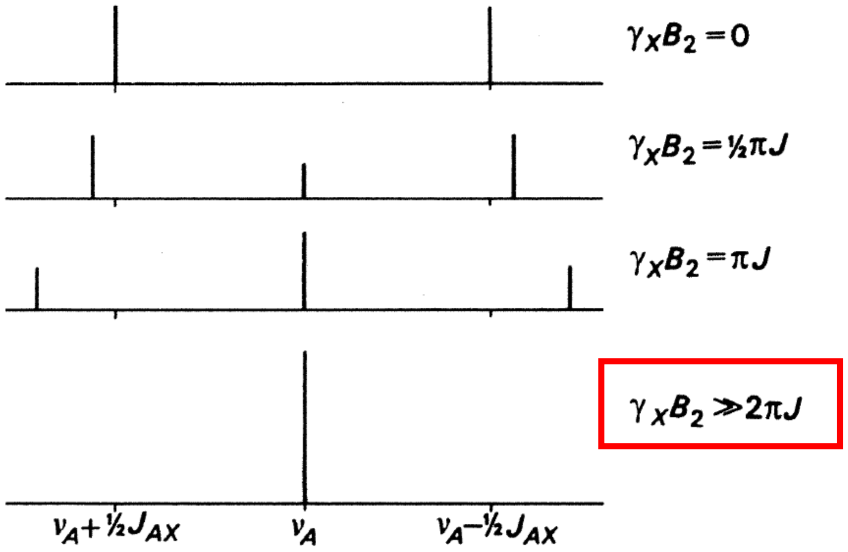

Harris, R.K (1986), Nuclear Magnetic Resonance Spectroscopy

DECOUPLING SCHEMES

- Continuous wave (narrow band, on resonance decoupling)
- Increase decoupling bandwidth
  - 'spin-flip' decoupling

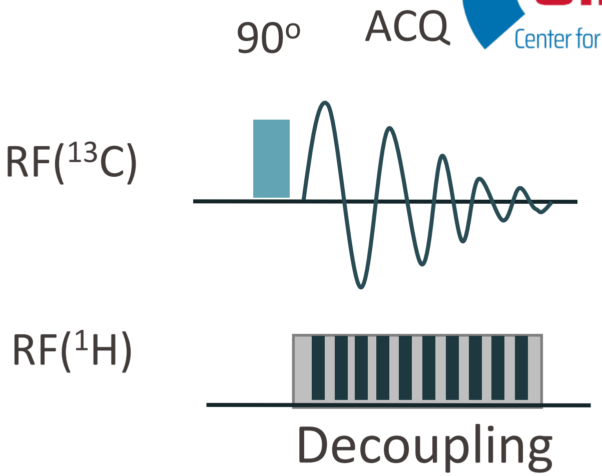

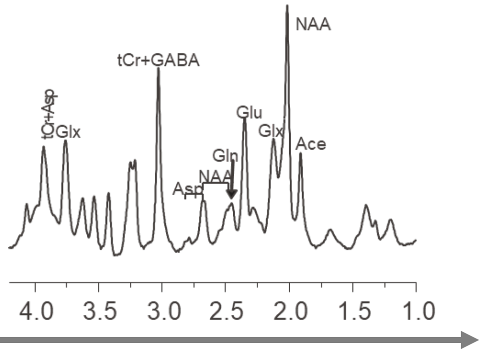

Δf=1200Hz

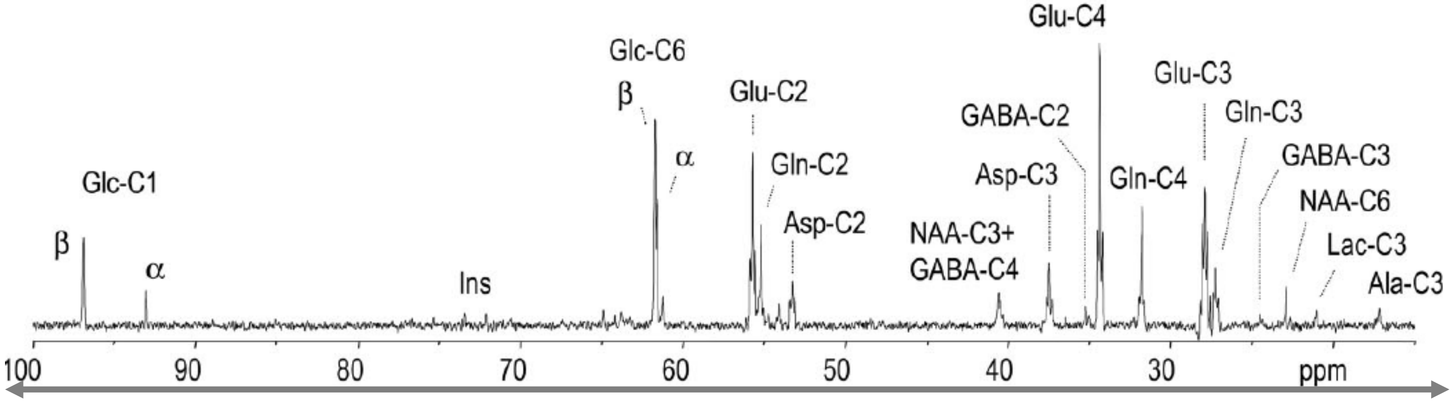

Δf= 7500Hz

7T

Freeman et al , NMR Biomed,10, (1997)

DECOUPLING SCHEMES

- Composite pulses
  - MLEV (Modulated Low-power Evolution): $90^o(x)\ 180^o(y)\ 90^o(x)$
  - WALTZ: $90^o(x)\ 180^o(-x)\ 270^o(x) = 1\bar{2}3$

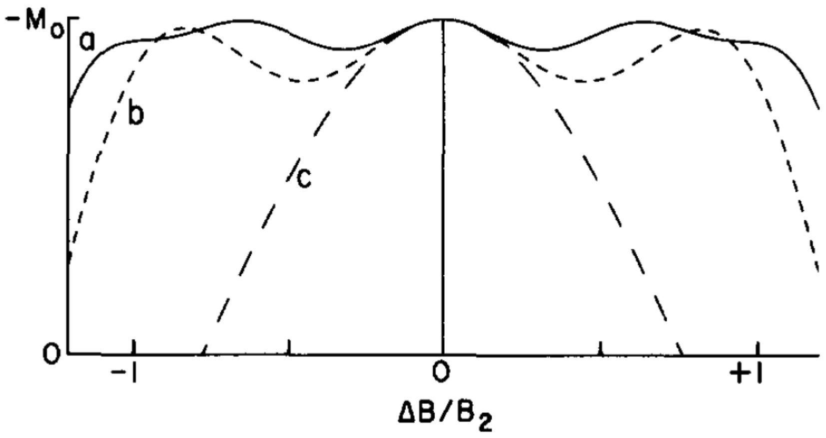

resonance offset

a. WALTZ
b. MLEV
c. $180^o(x)$

Levitt et al., J. Magn. Reson. 33, 1979.
Shaka et al , J Magn Reson, 52,1983.

DECOUPLING: BW VS SPECIFIC ABSORPTION RATE

- Efficient decoupling: the desired decoupling bandwidth with the lowest possible RF power

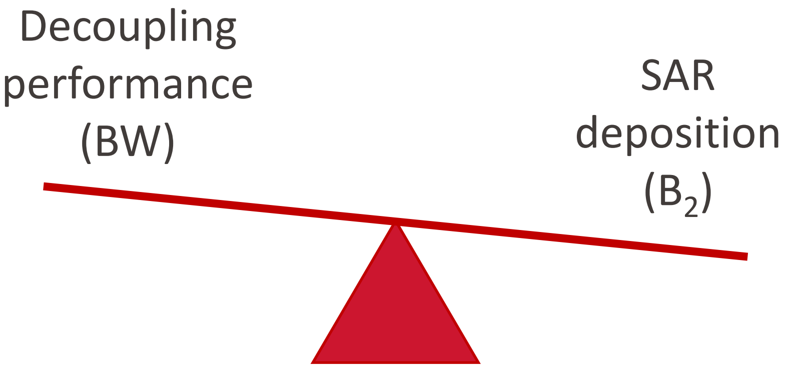

IEC (International Electrotechnical Commission):
3.2 W/kg (head) or 10 W/kg (body, over any 10g)

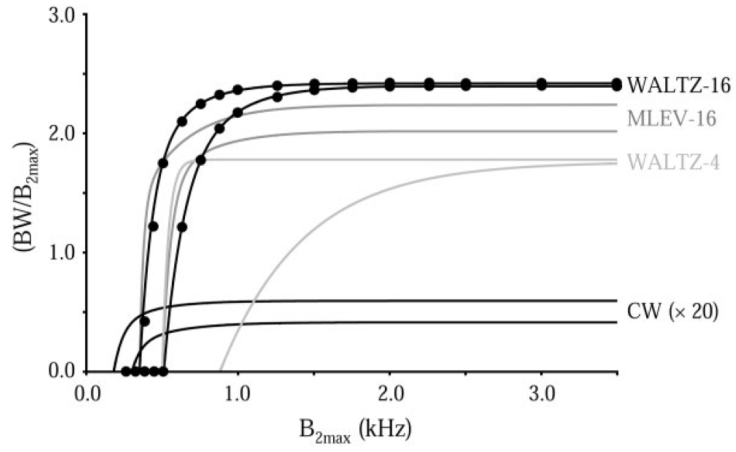

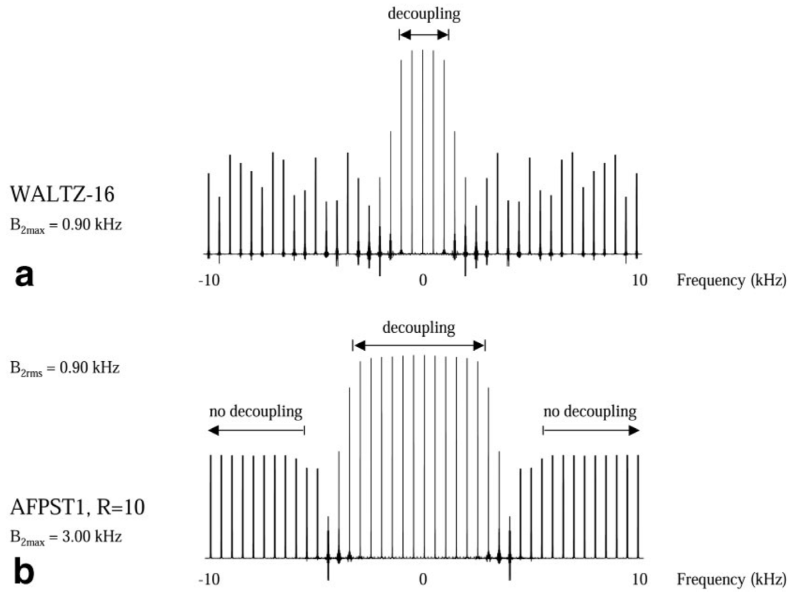

De graaf , Magn Reson Med, 53,2005.

© CIBM | Center for Biomedical Imaging

Nuclear overhauser enhancement (NOE)

CIBM Center for Biomedical Imaging

- Albert Overhauser (1953)
- spin polarization transfer through dipolar cross-relaxation
- equilibrium magnetization of a given nucleus changes via RF irradiation of neighboring nuclei (induced by relaxation mechanism)

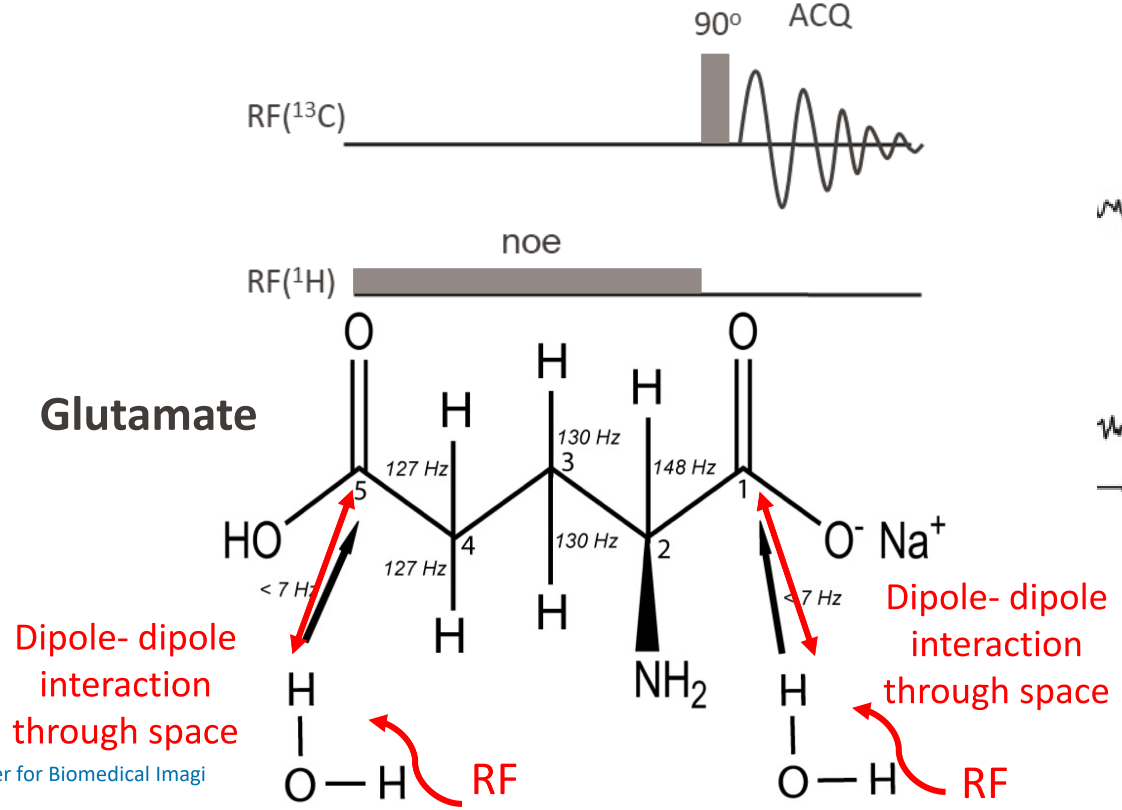

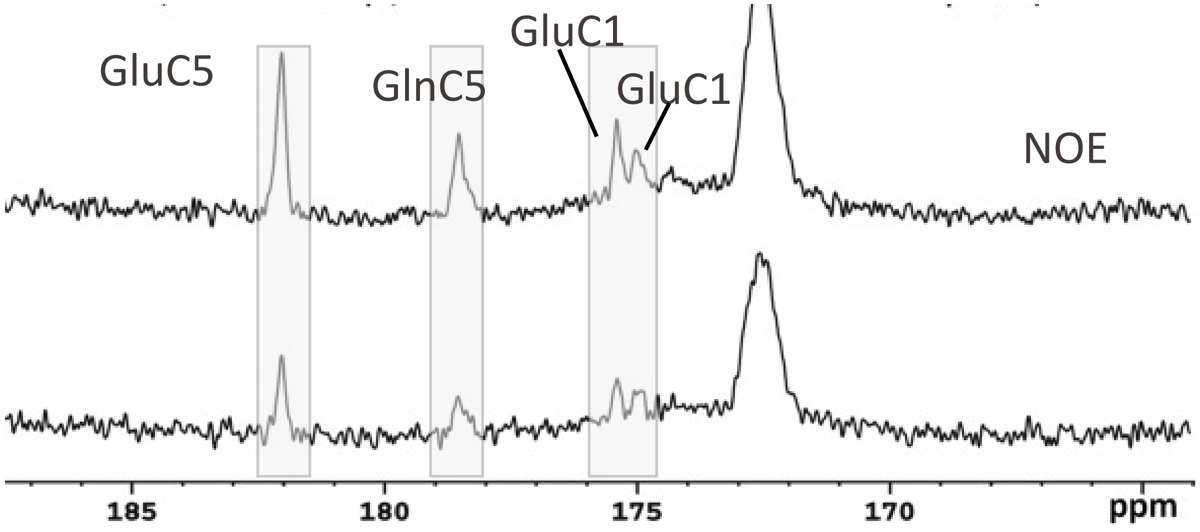

Li et al., MRM, 75:954–961, 2016

Sailasuta et al., J Magn Reson. 195: 219–225. 2008

© CIBM | Center for Biomedical Imagi

NOE FOR TWO-SPIN SYSTEM: I (^{13}C), S(^{1}H)

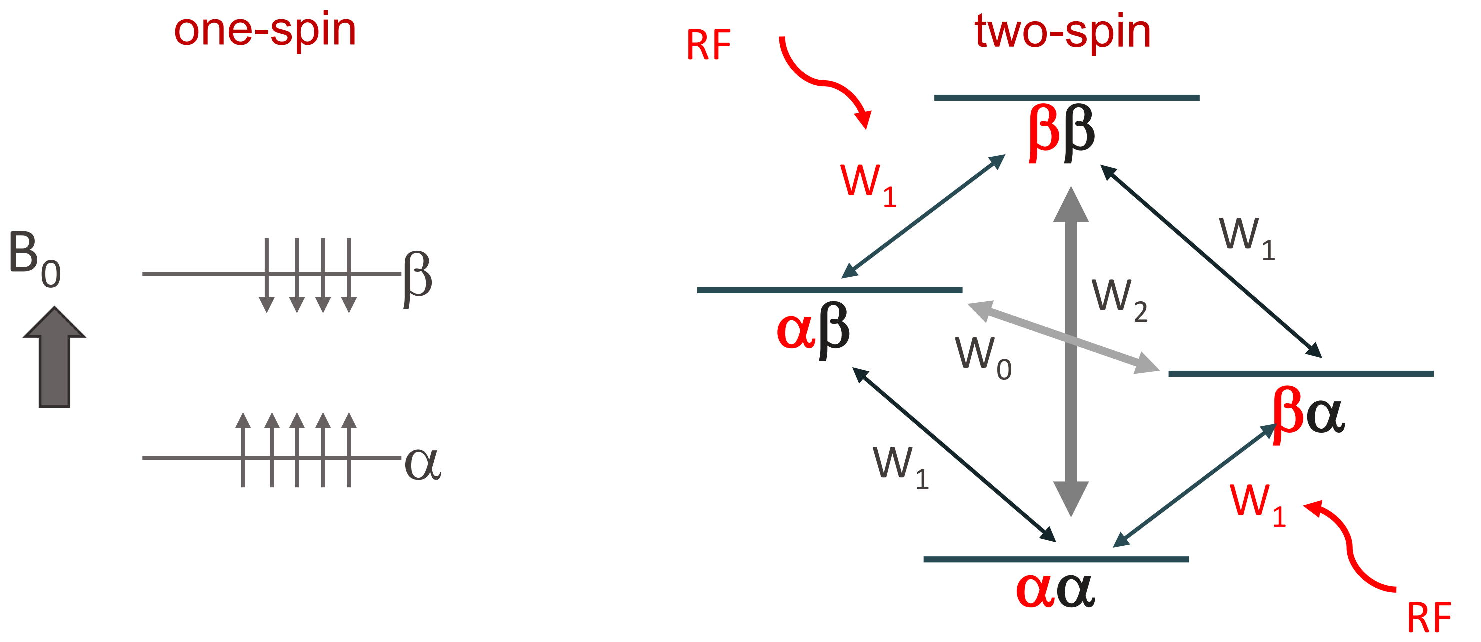

RF irradiation on $^{1}H \rightarrow$ changes equilibrium magnetization (population difference) of ^{13}C

- ✓ Relaxation is caused by random fluctuating magnetic fields due to the thermal motion of the molecules
- ✓ The fluctuating field induces **transitions** between the spin energy states

Transition probability W*:* probabilities/time that spins will change energy states (transition)

- W1: single quantum transition (flip of only one spin)
- W0: zero quantum transition (simultaneous flip of both spins in the opposite direction)
- W2: double quantum transition (simultaneous flip of both spins in the same direction)

© CIBM | Center for Biomedical Imaging

SUMMARY FOR NOE

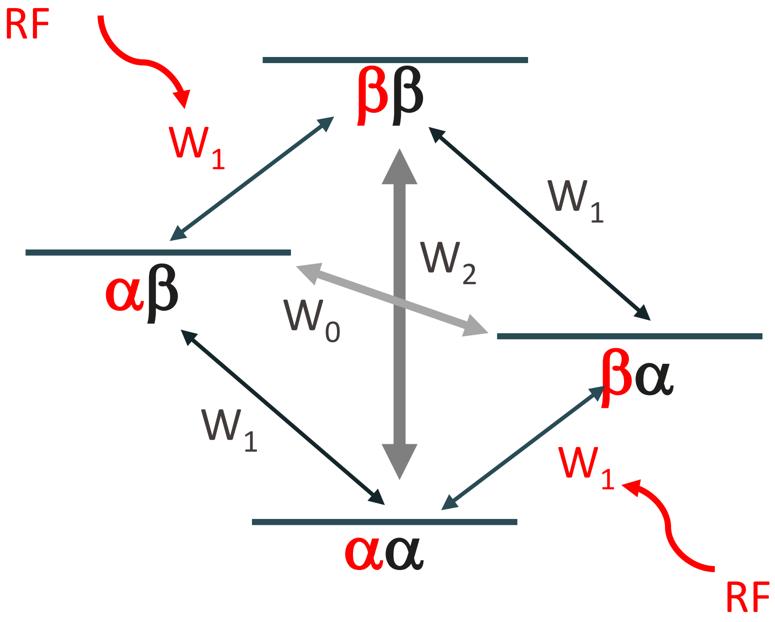

- An RF irradiation → saturation for one spin
- Mechanism: relaxation
- The enhancement depends on the contribution of relaxation mechanisms and molecules (e.g. the distance between spins)
  - W2: positive enhancement , W0: negative enhancement
- Experimental determination for NOE factor in vivo and in vitro
  - ^{31}P-^{1}H: 1.4-1.8
  - ^{13}C-^{1}H: 1.3-2.9

© CIBM | Center for Biomedical Imaging

POLARIZATION TRANSFER (INEPT AND DEPT)

INEPT

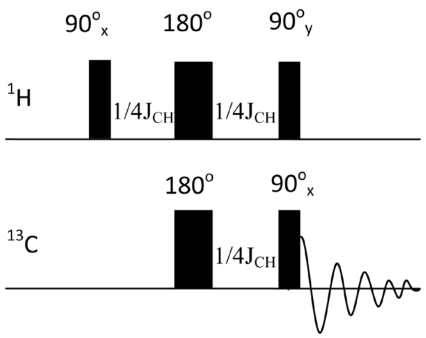

Refocused INEPT

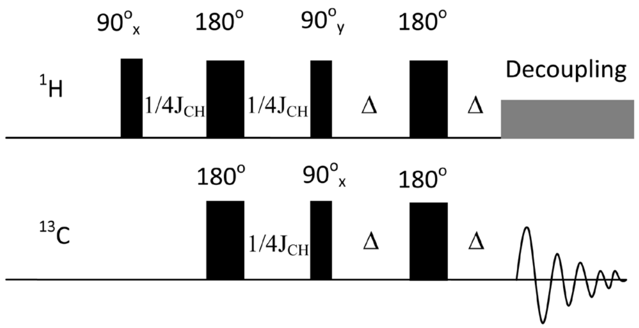

DEPT

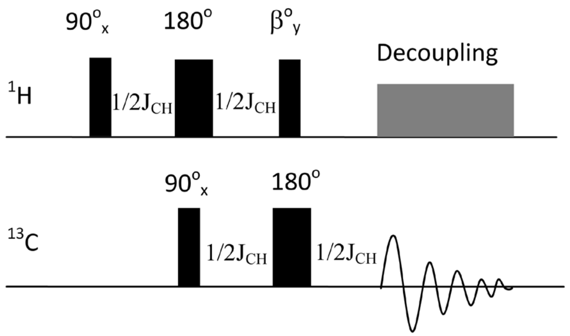

- INEPT: Insensitive Nuclei Enhanced by Polarization Transfer
- DEPT: Distortionless Enhancement by Polarization Transfer
- Polarization is transferred from a high γ nucleus to a low γ nucleus through J-coupling
- Enhancement by a factor of 4 (γ_{1H}/γ_{13C})

© CIBM | Center for Biomedical Imaging

INEPT

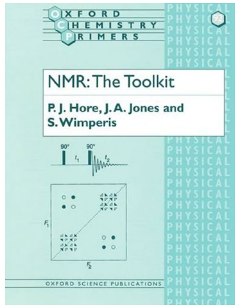

$\mathbf{I}_z, \mathbf{S}_z$	z magnetization(population difference)
$\mathbf{I}_x, \mathbf{I}_y, \mathbf{S}_x, \mathbf{S}_y$	in-phase magnetization in the $x' - y'$ plane
$2\mathbf{I}_x\mathbf{S}_z, 2\mathbf{I}_y\mathbf{S}_z, 2\mathbf{S}_x\mathbf{I}_z, 2\mathbf{S}_y\mathbf{I}_z$	antiphase magnetization in the $x' - y'$ plane
$2\mathbf{I}_x\mathbf{S}_y, 2\mathbf{I}_y\mathbf{S}_x, 2\mathbf{I}_x\mathbf{S}_x, 2\mathbf{I}_y\mathbf{S}_y$	zero-and double-quantum coherences (not observable)

INEPT

aI_z

bS_z

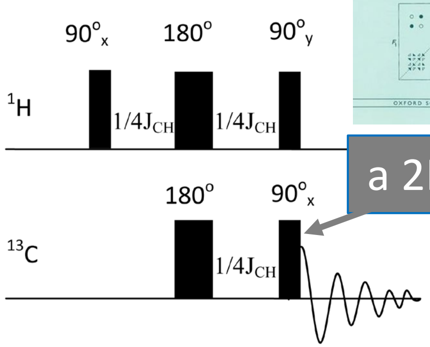

$a\ 2I_zS_y + b\ S_y$

$a=4b\ (\gamma_{1H=4}\gamma_{13C})$

CH

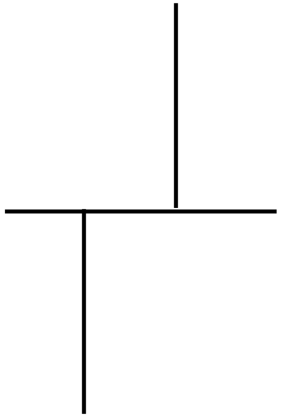

Decoupling
Enhancement
lost

Refocused INEPT

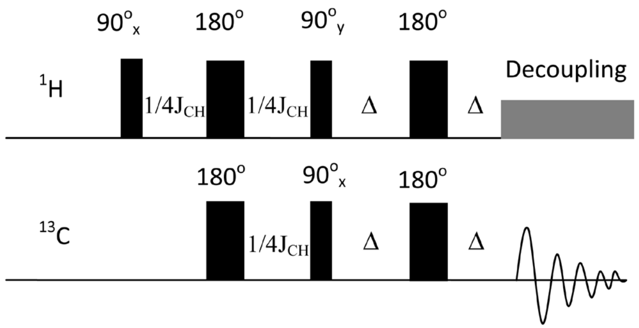

DEPT

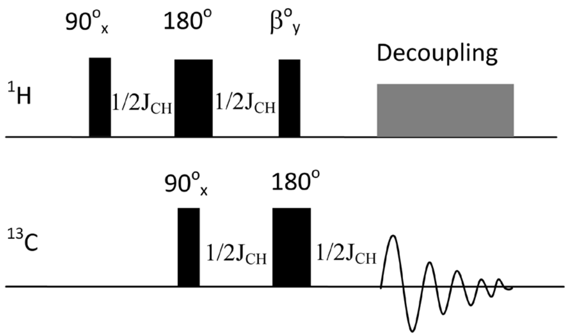

P.J. Hore, J.A.Jones, and S.Wimperis. NMR: The Toolkit. OUP Oxford, 2000

refocused INEPT AND DEPT

I_z, S_z	z magnetization(population difference)
I_x, I_y, S_x, S_y	in-phase magnetization in the $x' - y'$ plane
$2I_xS_z, 2I_yS_z, 2S_xI_z, 2S_yI_z$	antiphase magnetization in the $x' - y'$ plane
$2I_xS_y, 2I_yS_x, 2I_xS_x, 2I_yS_y$	zero-and double-quantum coherences (not observable)

Refocused INEPT

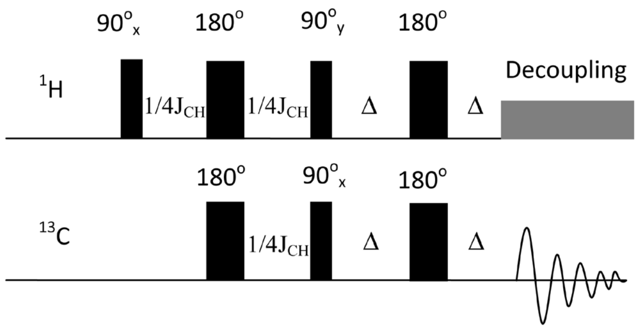

a=4b ($\gamma_{1H=4}\gamma_{13C}$)

	Δ	1/4J	1/2J	3/4J
CH	$S_x\sin(\pi J\Delta)$	0.707	1	0.707
CH_2	$2S_x\sin(\pi J\Delta)\cos(\pi J\Delta)$	1	0	-1
CH_3	$3S_x\sin(\pi J\Delta)\cos^2(\pi J\Delta)$	1.061	0	1.061

DEPT

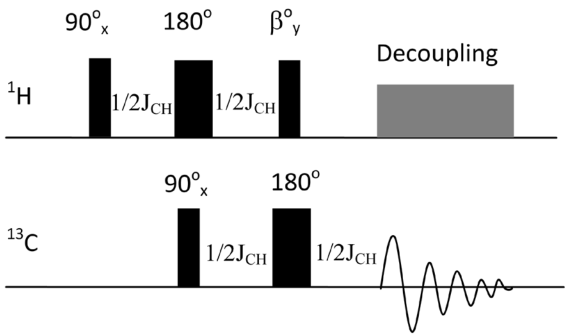

	β	45º	90º	135º
CH	$S_x\sin\beta$	0.707	1	0.707
CH_2	$2S_x\sin\beta\cos\beta$	1	0	-1
CH_3	$3S_x\sin\beta\cos^2\beta$	1.061	0	1.061

© CIBM | Center for Biomedical Imaging

P.J. Hore, J.A.Jones, and S.Wimperis. NMR: The Toolkit. OUP Oxford, 2000

PT+^{1}H LOCALIZATION

- ^{1}H localization with PT: long T_2 metabolites
  - Localization with ^{1}H magnetization: CSDE ↓

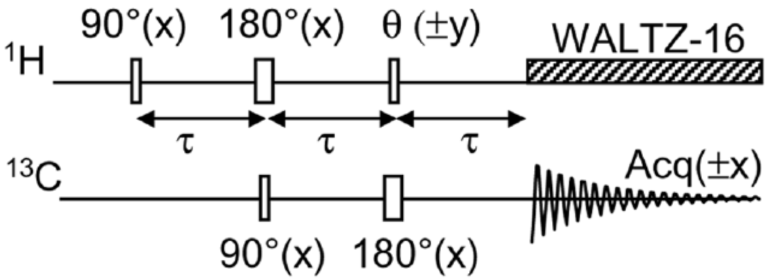

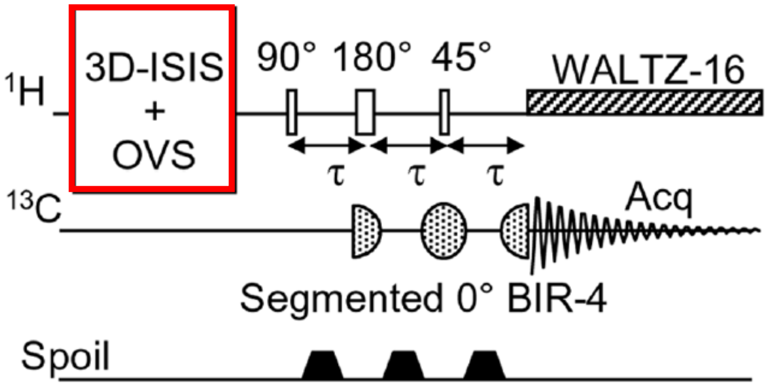

Henry et al., ., Magn Reson Med , 50:684–692 (2003)

$$\text{CSDE (\%)}: \frac{\Delta x}{x} = \frac{\Delta f}{BW}$$

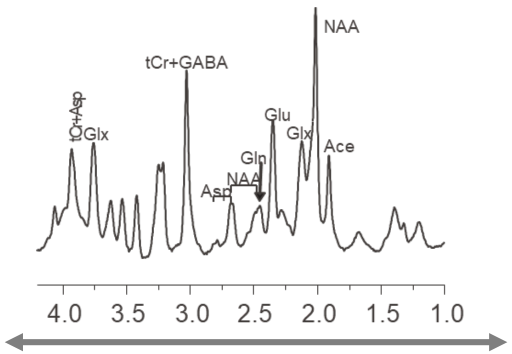

Δf=1200Hz

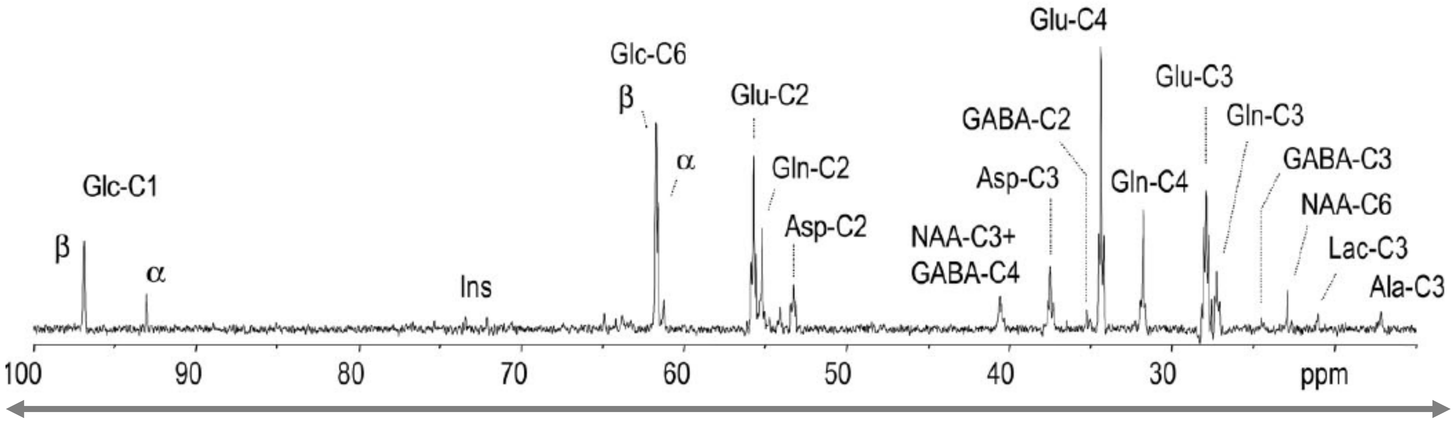

Δf= 7500Hz

Heteronuclear editing (Indirect detection)

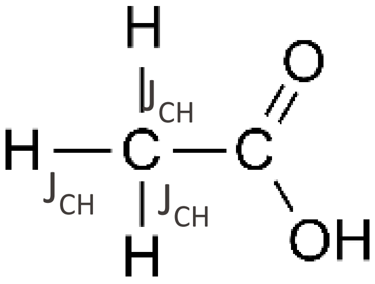

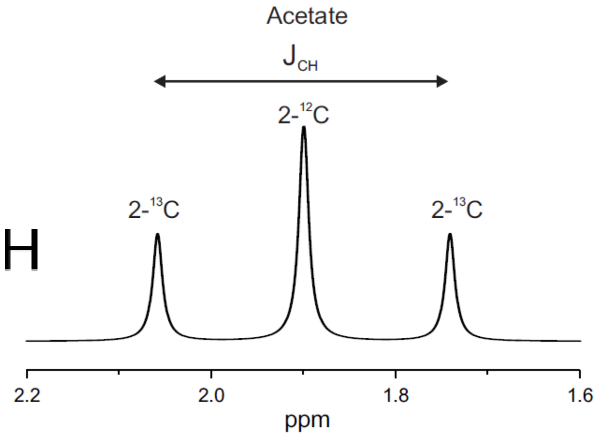

- Detect ^{1}H resonances bound to ^{13}C
- Higher sensitivity x 16 ($\gamma_{1H}=4\gamma_{13C}$) $\mathbf{M}_0 = N_s \frac{\gamma^2 \hbar^2 B_0}{4kT} \mathbf{k}$

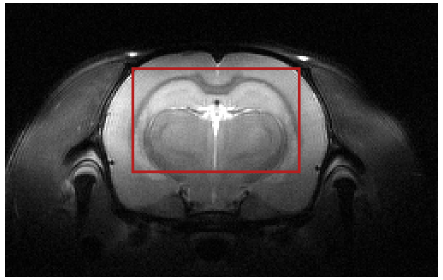

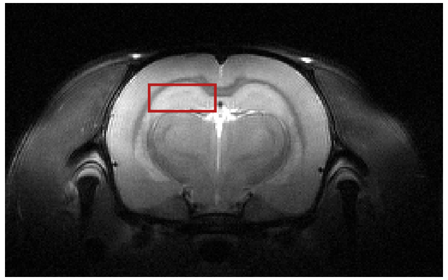

- Direct measurement of fractional enrichment [$FE={}^{13}C/({}^{13}C+{}^{12}C)$]
- Heteronuclear editing: J-difference editing
- limitation: narrow spectral resolution in ^{1}H

J-DIFFERENCE EDITING

Proton-Observed Carbon-Edited Spectroscopy (POCE)

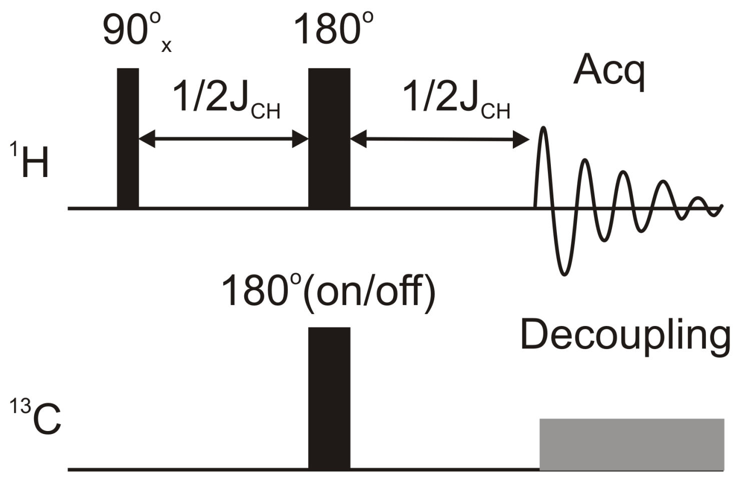

J_{CH}=120-140Hz
TE=7-8ms

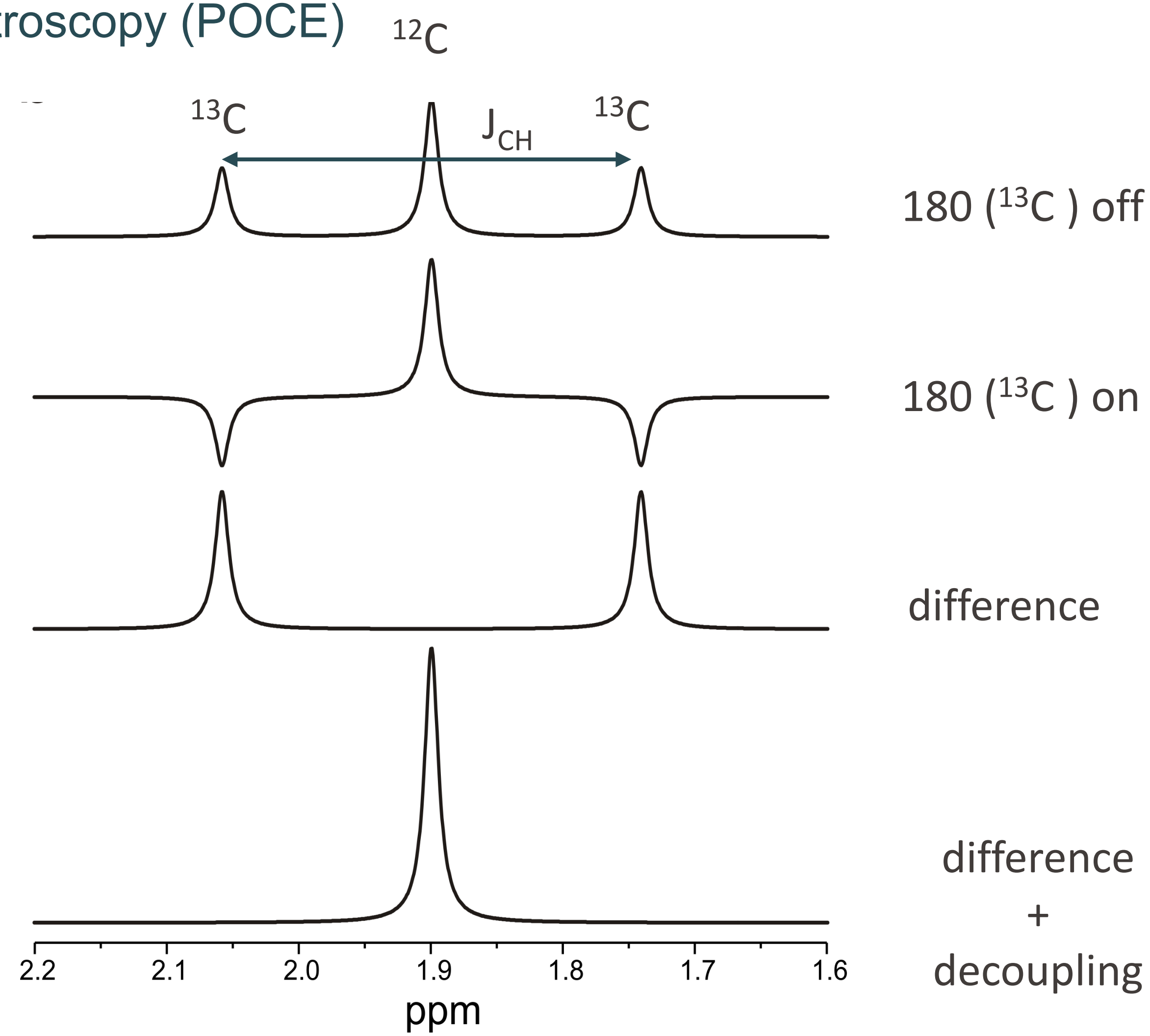

COMPARISON OF DIRECT AND INDIRECT ^{13}C MRS

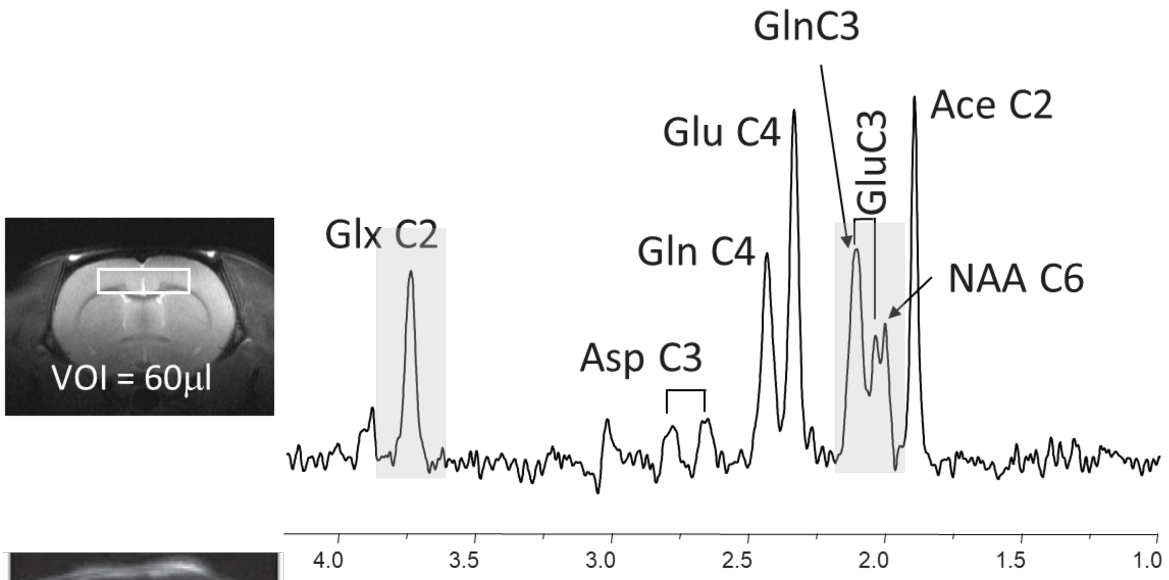

- ☺ High sensitivity (high temporal and spatial resolution)
- ☺ total metabolite concentrations (13C+12C)
- ☹ Limited spectral resolution-> limited metabolic info

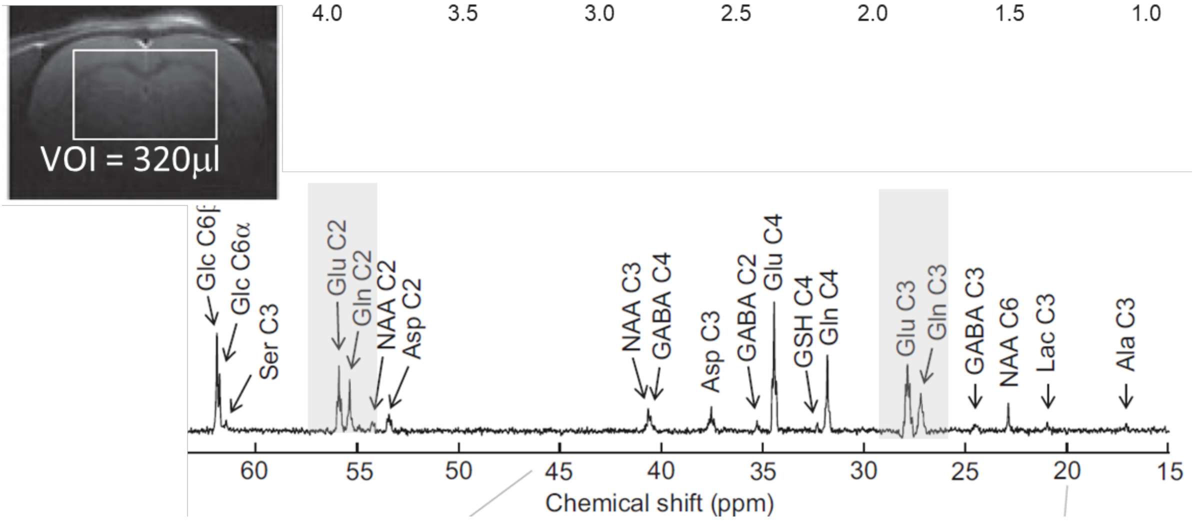

- ☺ High spectral resolution-> large metabolic info
- ☹ Low sensitivity (limited temporal and spatial resolution)
- ☹ Additional measurement for metabolite concentration

Xin et al. Magn Reson Med 64,2010. Durate et al., J. Neurochem.126,2013.

HYPERPOLARIZED ^{13}C MRS

Dissolution DNP

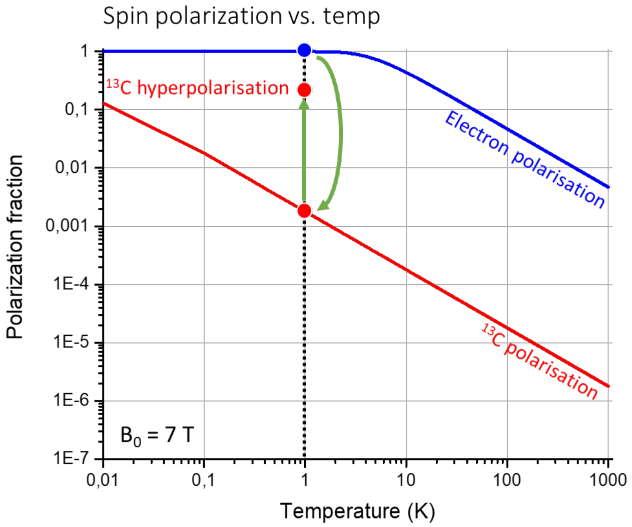

Carver et al., Phys. Rev. (1953)

microwaves

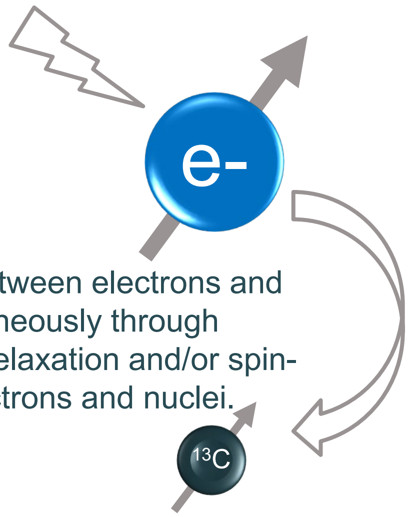

polarization transfers between electrons and nuclei can occur spontaneously through electron-nuclear cross-relaxation and/or spin-state mixing among electrons and nuclei.

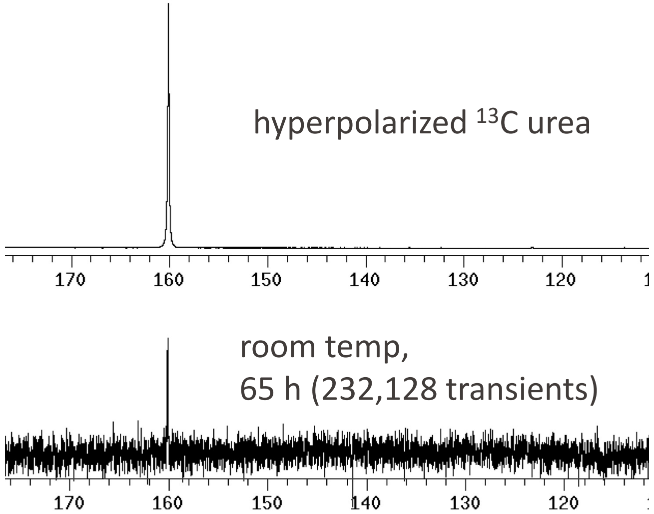

Ardenkjær-Larsen et al., PNAS (2003)

- loss of the polarization back to thermal equilibrium
- short measurement window limited by T_1
- a compound with long T1 is favorable for DNP experiments

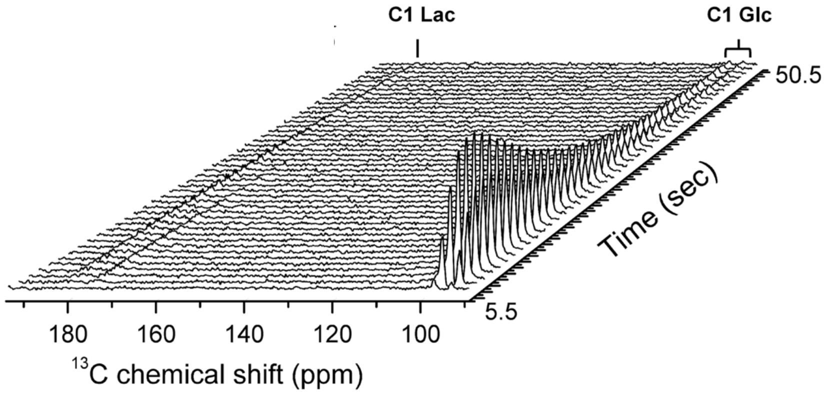

Mishkovsky et al., Sci. Rep. (2017)

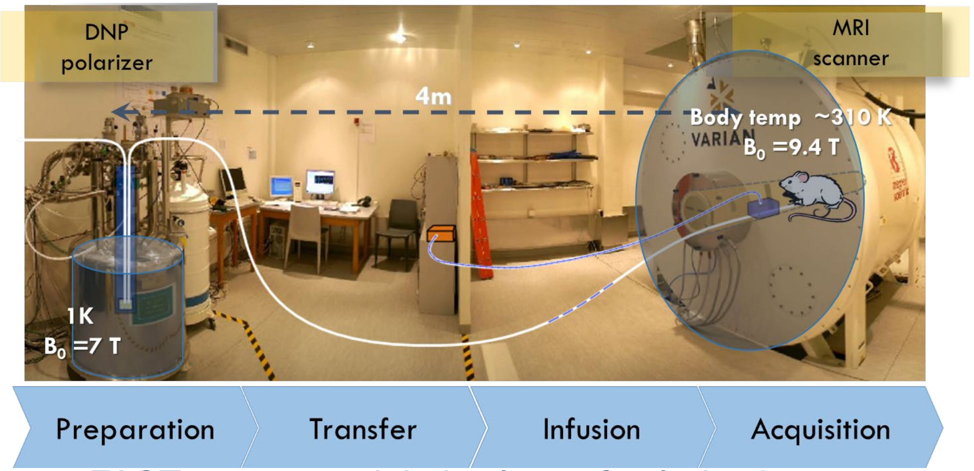

FAST process: minimize loss of polarization

Courtesy of M. Mishkovsky

© CIBM | Center for Biomedical Imaging

HP ^{13}C MRS APPLICATION IN PROSTATE CANCER

Hyperpolarized [1-^{13}C]Pyruvate

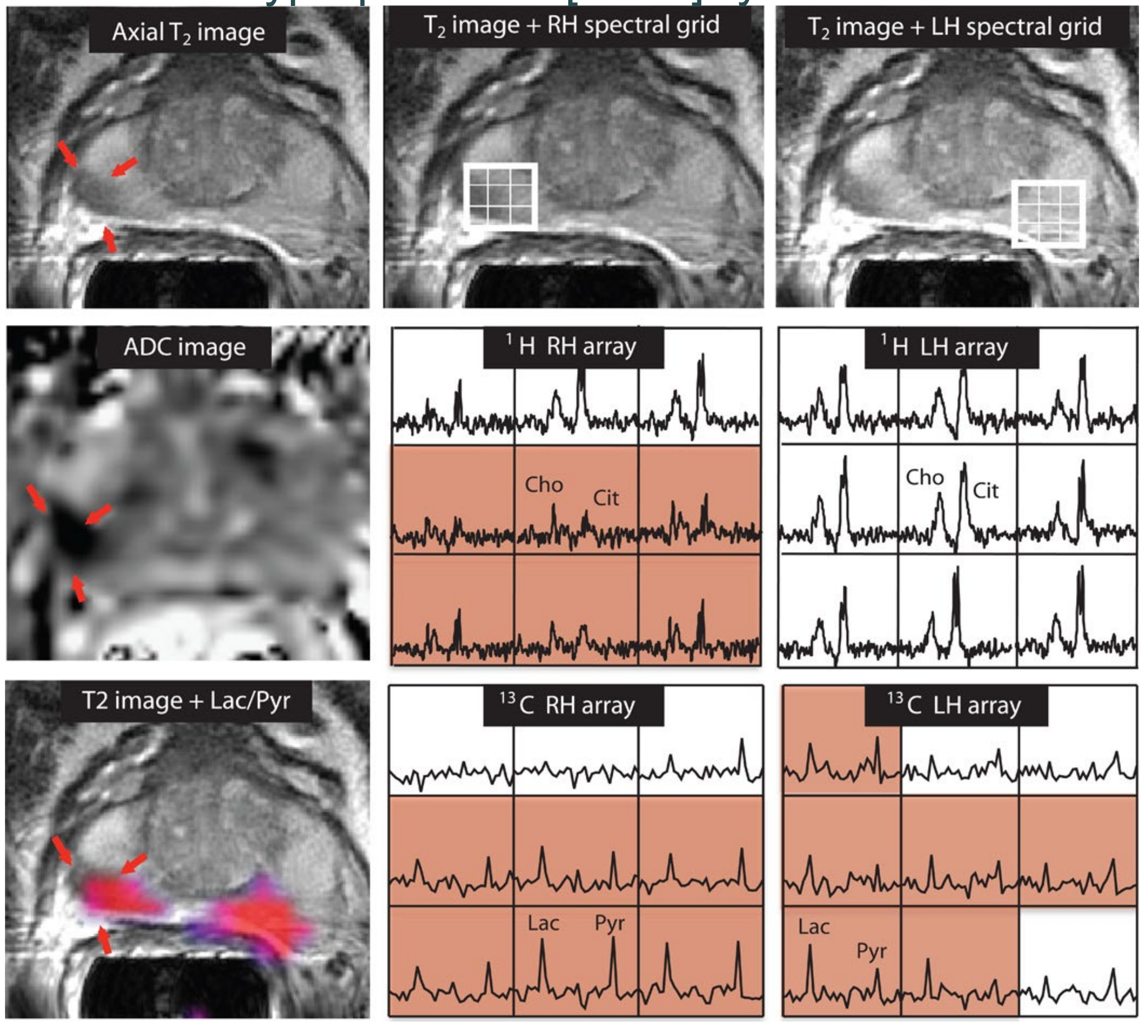

prostate cancer: ^{1}H MRSI reduced citrate and elevated choline/citrate

HP ^{13}C could detect affected areas that are negative in MRI images and ^{1}H MRSI.

Nelson et al, Science Translational Medicine, (2013)

SUMMARY

- Multinuclear MRS (^{1}H, ^{2}H, ^{13}C, ^{31}P, ^{17}O etc): a valuable tool to study brain metabolism
  - metabolite levels
  - chemical reaction rates
  - kinetics in metabolic pathway (e.g. CMR glc, TCA cycle and neurotransmitter cycling fluxes)

- Challenges in clinical implementation
  - low sensitivity, limited spatial resolution
  - long scanning time
  - stringent RF deposition regulations

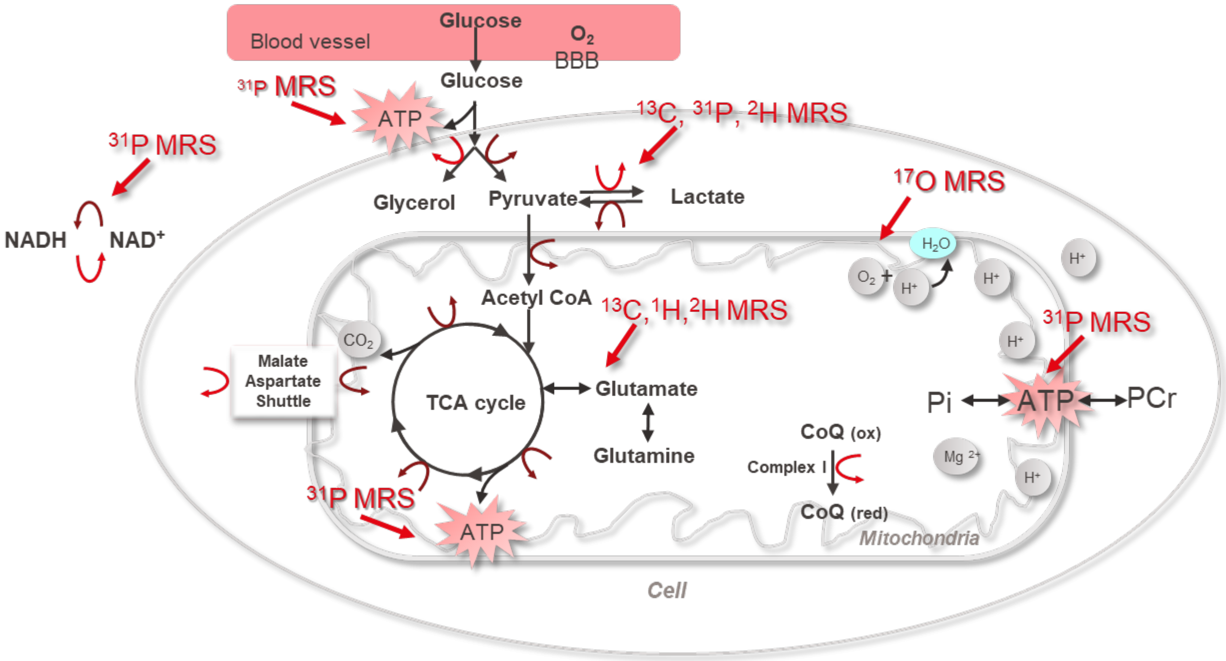

THANK YOU FOR YOUR ATTENTION